Exploring the Mechanism of Aqueous C−H Activation by Pt(II) through Model Chemistry: Evidence for the Intermediacy of Alkylhydridoplatinum(IV) and Alkane σ-Adducts

Shannon S. Stahl, Jay A. Labinger,* and John E. Bercaw*

Contribution from the Arnold and Mabel Beckman Laboratories of Chemical Synthesis, California Institute of Technology, Pasadena, California 91125

Received January 12, 1996[⊗]

Abstract: The protonolysis mechanisms of several alkylplatinum(II) complexes [(tmeda)PtMeCl (**2**) (tmeda = *N*,*N*,*N*′,*N*′-tetramethylethylenediamine), (tmeda)Pt(CH_2Ph)Cl (**5**), (tmeda)$PtMe_2$ (**11**), and *trans*-$(PEt_3)_2Pt(CH_3)Cl$ (**15**)] in CD_2Cl_2 and CD_3OD have been investigated. These reactions model the microscopic reverse of C−H activation by aqueous Pt(II). Each of the four systems (**2** in CD_3OD, **5** in CD_2Cl_2, **11** in CD_3OD, and **15** in CD_3OD) exhibits different behavior in the protonolysis reaction as observed by low-temperature ^1H NMR spectroscopy. Protonolysis of **2** in methanol-d_4 proceeds with no observable intermediates. Reversible reaction between **5** and HCl in CD_2Cl_2 at −78 °C produces (tmeda)Pt(CH_2Ph)(H)Cl_2 (**6**), which undergoes reductive elimination of toluene at higher temperatures. Treatment of **11** with HCl in methanol at −78 °C generates (tmeda)$PtMe_2$(H)Cl (**12**), which incorporates deuterium from solvent (CD_3OD) into the methyl groups prior to reductive elimination of methane. Finally, **15** reacts with H^+ in methanol to liberate methane with no intermediates observed. However, hydrogen/deuterium exchange takes place between the solvent (CD_3OD) and Pt−Me prior to methane loss. Each of these reactions was evaluated further to determine the kinetics of the reaction, activation parameters, and isotope effects. Based on the results, a common mechanistic sequence is proposed to operate in all the reactions: (1) chloride- or solvent-mediated protonation of Pt(II) to generate an alkylhydridoplatinum(IV) intermediate, (2) dissociation of solvent or chloride to generate a cationic, five-coordinate platinum(IV) species, (3) reductive C−H bond formation producing a platinum-(II) alkane σ-complex, and (4) loss of alkane either through an associative or dissociative substitution pathway. The characteristics of each system differ due to changes in the relative stabilities of the intermediates and/or transition states upon varying the solvent or alkylplatinum species.

Identifying practical routes to alkane functionalization continues to be actively pursued.[1−3] Although many organometallic systems have been identified which selectively *activate* C−H bonds, most rely on the generation of a high-energy, reactive intermediate which decomposes rapidly if exposed to oxidants necessary for catalytic turnover. Recently, several promising, rather robust systems have been developed based on late transition metals (e.g., Pd, Pt, and Hg).[4−7] These metal complexes undergo electrophilic activation and subsequent oxidation of alkanes. The first such homogeneous alkane oxidation system was discovered by Shilov and co-workers >20 years ago;[8] it utilized a mixture of Pt(II) and Pt(IV) salts in aqueous solution to convert methane to mixtures of methanol and methyl chloride. Although various features have thus far prevented its practical utility, this system remains one of few examples of catalytic (in Pt(II)) routes to alkane functionalization. Recently, we[9−12,21] and others[13−20] have been exploring some of the mechanistic features of this system in order to better understand this remarkable reactivity.

In agreement with Shilov's original proposal,[13] we believe the catalytic mechanism consists of three primary transformations (Scheme 1): (1) electrophilic activation of the alkane by Pt(II) to generate an alkylplatinum(II) intermediate, (2) two-electron oxidation of alkylplatinum(II) to generate an alkylplatinum(IV) species, and (3) reductive elimination of R−X (X = Cl or OH for example) to liberate the functionalized alkane and Pt(II) catalyst.

In recent years, we have elucidated several details related to the final two steps of the mechanism.[9−12] Unfortunately, very little is known about the nature of C−H activation, the step which appears to govern the overall rate as well as the

[⊗] Abstract published in *Advance ACS Abstracts,* June 1, 1996.

(1) Arndtsen, B. A.; Bergman, R. G.; Mobley, T. A.; Peterson, T. H. *Acc. Chem. Res.* **1995**, *28*, 154.
(2) *Selective Hydrocarbon Activation*; Davies, J. A., Watson, P. L., Liebman, J. F., and Greenberg, A., Eds.; VCH: New York, 1990.
(3) *Activation and Functionalization of Alkanes*; Hill, C. L., Ed.; John Wiley & Sons: New York, 1989.
(4) Gretz, E.; Oliver, T. F.; Sen, A. *J. Am. Chem. Soc.* **1987**, *109*, 8109.
(5) Kao, L.-C.; Hutson, A. C.; Sen, A. *J. Am. Chem. Soc.* **1991**, *113*, 700.
(6) Labinger, J. A.; Herring, A. M.; Bercaw, J. E. *J. Am. Chem. Soc.* **1990**, *112*, 5628.
(7) Periana, R. A.; Taube, D. J.; Evitt, E. R.; Loffler, D. G.; Wentrcek, P. R.; Voss, G.; Masuda, T. *Science* **1993**, *259*, 340.
(8) Goldshleger, N. F.; Eskova, V. V.; Shilov, A. E.; Shteinman, A. A. *Zh. Fiz. Khim.* **1972**, *46*, 1353.
(9) Labinger, J. A.; Herring, A. M.; Lyon, D. K.; Luinstra, G. A.; Bercaw, J. E.; Horvath, I. T.; Eller, K. *Organometallics* **1993**, *12*, 895.
(10) Luinstra, G. A.; Labinger, J. A.; Bercaw, J. E. *J. Am. Chem. Soc.* **1993**, *115*, 3004.
(11) Luinstra, G. A.; Wang, L.; Stahl, S. S.; Labinger, J. A.; Bercaw, J. E. *Organometallics* **1994**, *13*, 755.
(12) Luinstra, G. A.; Wang, L.; Stahl, S. S.; Labinger, J. A.; Bercaw, J. E. *J. Organomet. Chem.* **1995**, *504*, 75.
(13) Kushch, L. A.; Lavrushko, V. V.; Misharin, Y. S.; Moravsky, A. P.; Shilov, A. E. *Nouv. J. Chim.* **1983**, *7*, 729.
(14) Horvath, I. T.; Cook, R. A.; Millar, J. M.; Kiss, G. *Organometallics* **1993**, *12*, 8.
(15) Sen, A.; Lin, M.; Kao, L.-C.; Hutson, A. C. *J. Am. Chem. Soc.* **1992**, *114*, 6385.
(16) Sen, A.; Benvenuto, M. A.; Lin, M.; Hutson, A. C.; Basickes, N. *J. Am. Chem. Soc.* **1994**, *116*, 998.
(17) Hutson, A. C.; Lin, M.; Basickes, N.; Sen, A. *J. Organomet. Chem.* **1995**, *504*, 69.
(18) Zamashchikov, V. V.; Litvinenko, S. L.; Uzhik, O. N.; Galat, V. F. *Zh. Obs. Khim.* **1986**, *56*, 2417.
(19) Zamashchikov, V. V.; Popov, V. G.; Litvinenko, S. L. *Izv. Akad. Nauk SSSR, Ser. Khim.* **1993**, *42*, 389.
(20) Zamashchikov, V. V.; Popov, V. G.; Rudakov, E. S.; Mitchenko, S. A. *Dokl. Akad. Nauk SSSR* **1993**, *333*, 34.

S0002-7863(96)00110-2 CCC: $12.00

Scheme 1

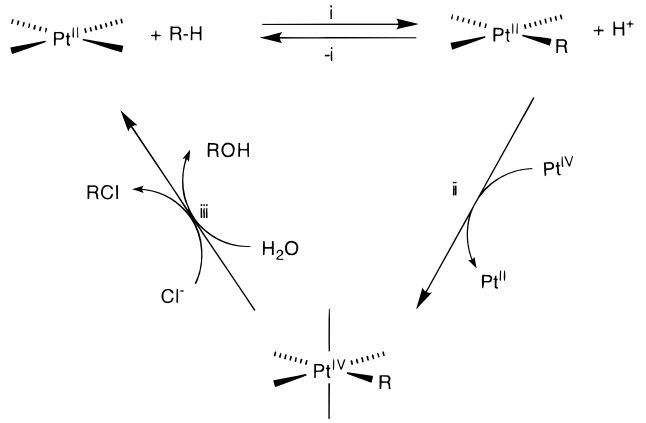

selectivity of the catalytic cycle. Recently we have been attempting to delineate some of the mechanistic features of this reaction.

Two possible pathways have been proposed for C−H activation leading to an alkylplatinum(II) intermediate:[9,22−24] (1) oxidative addition of the C−H bond at Pt(II) yielding an alkylhydridoplatinum(IV) species which is subsequently deprotonated (eq 1) or (2) deprotonation of an intermediate Pt(II)−alkane σ-complex (eq 2). Neither intermediate has been observed directly.

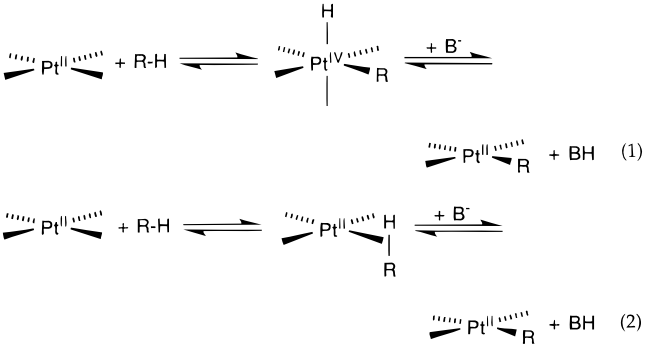

In the course of our investigations, we have encountered difficulties exploring direct reactions of aqueous Pt(II) salts with alkanes. Even in the absence of Pt(IV), oxidation products are generated with immediate precipitation of platinum metal, accompanied by extensive H/D exchange between alkanes and deuterated solvent. Unlike previous reports,[22,25] we have *not* observed H/D exchange prior to formation of Pt(0).

We subsequently began investigating the microscopic reverse of the C−H activation step, namely protonolysis of alkylplatinum(II) species. The catalytic intermediate, $[Cl_3Pt^{II}CH_3]^{2-}$ (**1**), is presumed to be generated upon 2e$^-$ reduction of $[Pt^{IV}MeCl_5]^{2-}$, however **1** immediately liberates methane when the reaction is carried out in a protic solvent (i.e., CH_3OH and H_2O). Furthermore, in aprotic media we found that **1** is unstable with respect to disproportionation into $[PtCl_4]^{2-}$ and $[Cl_2Pt^{II}(CH_3)_2]^{2-}$.[12,26]

Related alkylplatinum(II) model complexes containing stabilizing donor ligands (e.g., amines or phosphines) proved more amenable to study. Protonolysis studies of such complexes have been conducted by other groups in the past; however, several different mechanisms have been proposed.[27−31] Furthermore, when we began our work, no intermediates had been identified in such reactions, and thus mechanistic proposals were based on less direct evidence such as rate laws, isotope effects, or competition studies. Recently, however, three groups have independently identified the presence of alkylhydridoplatinum(IV) intermediates in the protonolysis of alkylplatinum(II) species in organic solvents.[21,32−34] We report herein studies of the protonolysis reaction intended to examine the viability of alkane adducts (σ-complexes) and/or alkylhydridoplatinum(IV) species as intermediates in alkane activation by Pt(II) in aqueous solution.

Results

Protonolysis of (tmeda)Pt(CH$_3$)Cl (2) (tmeda = *N,N,N′,N′*-Tetramethylethylenediamine) in Methanol. The protonolysis of (tmeda)Pt(CH_3)Cl (**2**) with HCl in methanol proceeds cleanly to generate (tmeda)$PtCl_2$ and methane (eq 3).

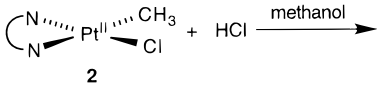

2

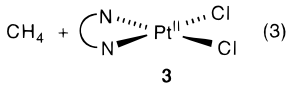

3

Monitoring the reaction at low temperature (−50 to −25 °C) in CD_3OD by ^{1}H NMR spectroscopy reveals pseudo-first-order kinetics for the conversion of **2** to (tmeda)$PtCl_2$ (**3**); *no intermediates are observed*.[35] The rate is first order in both hydrogen ion and chloride concentration (Figures 1 and 2, respectively) at constant ionic strength (μ = 1.0 M = [HOTf] + [$LiClO_4$] + [LiCl]) over the concentration ranges [HOTf] = 0 to 0.38 M and [Cl$^-$] = 0.13 to 0.66 M. Significantly, the dependence on chloride exhibits a non-zero intercept (Figure 2). Activation parameters were determined from an Eyring plot: $\Delta H^{\ddagger} = 19.4 \pm 1.5$ kcal·mol^{-1} and $\Delta S^{\ddagger} = 14 \pm 5$ eu.[36]

Protonolysis of **2** with LOTf (L = H, D) in a 19.3:1 mixture of CD_3OD:CD_3OH at 0 °C generates a mixture of methane isotopomers, CH_4:CH_3D = 1:2.13, leading to a kinetic deuterium

(21) Stahl, S. S.; Labinger, J. A.; Bercaw, J. E. *J. Am. Chem. Soc.* **1995**, *117*, 9371.
(22) Shilov, A. E. *Activation of Saturated Hydrocarbons by Transition Metal Complexes*; Reidel: Dordrecht, 1984.
(23) Shilov, A. E. In *Activation and Functionalization of Alkanes*; Hill, C. L., Ed.; John Wiley & Sons: New York, 1989; p 1.
(24) Crabtree, R. H. *Chem. Rev.* **1995**, *95*, 987.
(25) Goldshleger, N. F.; Tyabin, M. B.; Shilov, A. E.; Shteinman, A. A. *Zh. Fiz. Khim.* **1969**, *43*, 2174.
(26) Wang, L.; Stahl, S. S.; Labinger, J. A.; Bercaw, J. E. *J. Mol. Catal.* In press.
(27) Belluco, U.; Giustiniani, M.; Graziani, M. *J. Am. Chem. Soc.* **1967**, *89*, 6494.
(28) Alibrandi, G.; Minniti, D.; Romeo, R.; Uguagliati, P.; Calligaro, L.; Belluco, U.; Crociani, B. *Inorg. Chim. Acta* **1985**, *100*, 107.
(29) Alibrandi, G.; Minniti, D.; Romeo, R.; Uguagliati, P.; Calligaro, L.; Belluco, U. *Inorg. Chim. Acta* **1986**, *112*, L15.
(30) Jawad, J. K.; Puddephatt, R. J.; Stalteri, M. A. *Inorg. Chem.* **1982**, *21*, 332.
(31) Siegbahn, P. E. M.; Crabtree, R. H. *J. Am. Chem. Soc.* **1996**, *118*, 4442.
(32) De Felice, V.; De Renzi, A.; Panunzi, A.; Tesauro, D. *J. Organomet. Chem.* **1995**, *488*, C13.
(33) Hill, G. S.; Rendina, L. M.; Puddephatt, R. J. *Organometallics* **1995**, *14*, 4966.
(34) Arylhydridoplatinum(IV) species have been identified previously: (a) Arnold, D. P.; Bennett, M. A. *Inorg. Chem.* **1984**, *23*, 2110. (b) Wehman-Ooyevaar, I. C. M.; Grove, D. M.; de Vaal, P.; Dedieu, A.; van Koten, G. *Inorg. Chem.* **1992**, *31*, 5484.
(35) Monitoring the reaction by UV−visible spectroscopy was attempted, but the product, (tmeda)$PtCl_2$, is insoluble and precludes the acquisition of reproducible data.
(36) Reaction conditions (Eyring plot for protonolysis of **2** in CD_3OD): [**2**] = 11.9 mM; [Cl$^-$] = 0 M; [H$^+$] = 0.18 M; μ = 1.18 M; temperature range −25 to −49 °C.

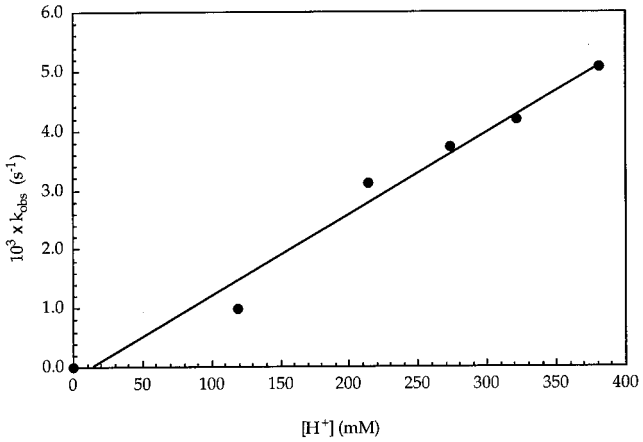

Figure 1. Plot of the [H^+] dependence of the rate of protonolysis of **2** in CD_3OD. [H^+] = 0−32 equiv; [**2**] = 11.9 mM; [Cl^-] = 0 M; μ = 1.0 M; temperature = −35 °C.

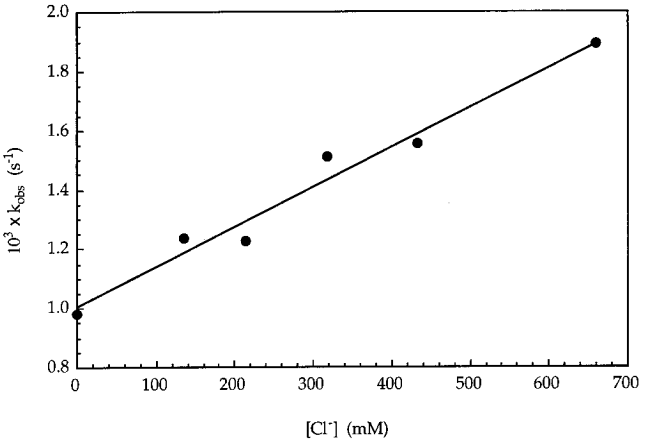

Figure 2. Plot of k_{obs} versus [Cl^-] for the protonolysis of **2** in CD_3OD. [Cl^-] = 0−55.4 equiv; [**2**] = 11.9 mM; [H^+] = 0.12 M; μ = 1.0 M; temperature = −35 °C.

isotope effect of 9.1 (±0.5). Comparing the pseudo-first-order rate constant for protonolysis of **2** in CD_3OH with HOTf (k_{obs} = 1.8 × 10^{-3} s^{-1}) versus CD_3OD with DOTf (k_{obs} = 0.77 × 10^{-3} s^{-1}) at −40 °C leads to a different isotope effect: k_H/k_D = 2.3 (±0.5).

Protonolysis of (tmeda)Pt(R)Cl (R = CH_3, CH_2Ph) in Methylene Chloride. Protonolysis of **2** also proceeds rapidly in dichloromethane at room temperature, releasing methane and also generating **3**. In contrast to reaction with HCl in methanol, addition of excess HCl (dissolved in diethyl ether-d_{10}) at −78 °C to a CD_2Cl_2 solution of **2** first results in oxidative addition to generate (tmeda)Pt(CH_3)(H)Cl_2 (**4**). Upon warming this solution to −60 °C, the reductive elimination of methane ensues along with formation of (tmeda)$PtCl_2$ (Scheme 2).

Although **4** is not sufficiently stable to isolate at room temperature, it has been characterized by ^{1}H NMR spectroscopy at low temperature (Table 1). The most distinctive characteristic is the platinum(IV) hydride resonance which appears far upfield (δ −23.6 ppm) with corresponding platinum satellites ($^1J_{^{195}Pt-H}$ = 1290 Hz, ^{195}Pt 33.8% natural abundance, S = $^1/_2$). These data are consistent with other Pt(IV) hydrides containing nitrogen and halide ligands.[32,33,37] The methyl resonance of **4** appears as a singlet (δ 1.6 ppm) with $^2J_{^{195}Pt-H}$ = 66.5 Hz.

The benzyl analog of **2**, (tmeda)Pt(CH_2Ph)Cl (**5**), reacts similarly with HCl, except the benzylhydridoplatinum(IV) complex (**6**) (Table 1) is more stable than **4**—toluene reductive elimination proceeds at −30 °C (Scheme 2). Consequently, this species was used to evaluate further mechanistic details. Oxidative addition of HCl to **5** is rapid and reversible: addition of DCl (as a diethyl ether-d_{10} solution) to **5** in CD_2Cl_2 at −78 °C produces **6**-d_1. Subsequent addition of a large excess of HCl results in the immediate appearance of the hydride resonance for **6** with no other spectroscopic changes.

Scheme 2

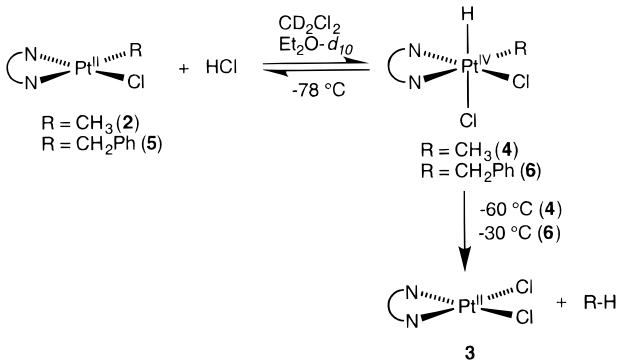

Reductive elimination of toluene follows a first-order dependence on [**6**]. The temperature dependence of the reductive elimination rates allowed determination of activation parameters: $\Delta H^‡$ = 14.0 ± 2.5 kcal·mol^{-1}, $\Delta S^‡$ = −18.5 ± 7.0 eu[38] (Figure 3). The rate of toluene formation from **6** is substantially increased by addition of Brönsted or Lewis acids (HCl, HOTf, $SnCl_4$), and in the case of triflic acid, the rate of reductive elimination of toluene is first order with respect to [HOTf] (0−263 mM; 0−20 equiv) (Figure 4). Moreover, direct protonation of **5** with HOTf (i.e., rather than addition of HOTf to a solution of **6**) at −80 °C proceeds immediately to toluene without evidence of (tmeda)Pt(CH_2Ph)(H)(Cl)(OTf). A series of experiments were carried out in which the [HOTf] was held constant (5 equiv relative to [**6**]) and the HCl concentration was varied between 0.11 and 0.62 M (9.4−51 equiv). As is apparent from Figure 5, toluene elimination is inhibited by added HCl. The dependence of the rate on chloride alone was also examined; however, surprisingly, the addition of tetrabutylammonium chloride to the reaction mixture results in immediate deprotonation of **6** and formation of **5** and tetrabutylammonium bichloride (eq 4).

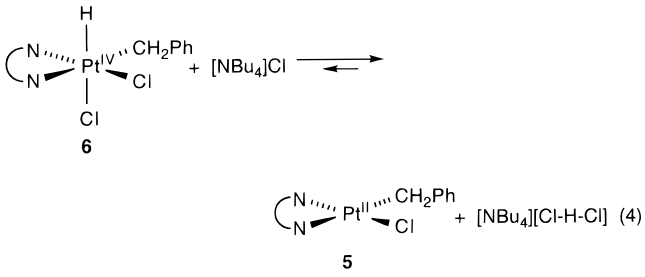

The presence of [NBu_4][Cl−H−Cl] was verified by comparing a solution FTIR spectrum of the reaction mixture to a solid-state infrared spectrum reported for [NMe_4][Cl−H−Cl].[39]

Integration of the the Pt^{IV}−*H* peak relative to one of the benzyl protons for **6** obtained by addition of a mixture of HCl and DCl to **5** reveals an *inverse* equilibrium deuterium isotope

(37) Wehman-Ooyevaar, I. C. M.; Grove, D. M.; de Vaal, P.; Dedieu, A.; van Koten, G. *Inorg. Chem.* **1992**, *31*, 5484.

(38) Reaction conditions (Eyring plot for reductive elimination of toluene from **6** in CD_2Cl_2): [**6**] = 13 mM; [HCl] = 65 mM; temperature range −24 to −43 °C.

(39) Two strong, very broad absorptions were observed at ∼1550 and 1000 cm^{-1}. Solid-state IR spectrum of [NMe_4][Cl−H−Cl]: Waddington, T. C. *J. Chem. Soc.* **1958**, 1708.

Table 1. Selected ^{1}H NMR Spectroscopic Data for Compounds Discussed in Text

compound	solvent	temp (°C)	peak assignment	chemical shift/ppm (multiplicity); coupling/Hz
(tmeda)Pt(CH_3)Cl (**2**)	CD_2Cl_2	25	Pt-C***H***$_3$	0.434 (s); $^2J_{Pt-H} = 78.9$
			Pt-N-C***H***$_3$	2.84 (s); $^3J_{Pt-H} = 51$
				2.70 (s); $^3J_{Pt-H} = <10$
			Pt-N-C***H***$_2$−	2.77 (m)
				2.54 (m)
(tmeda)Pt(CH_3)(H)Cl_2 (**4**)	CD_2Cl_2/Et_2O-d_{10} (10:1)	−70	Pt-C***H***$_3$	1.57 (s); $^2J_{Pt-H} = 66.5$
			Pt-***H***	−23.6 (s); $^1J_{Pt-H} = 1292$
			Pt-N-C***H***$_3$	3.02; $^3J_{Pt-H} \sim 57$
				2.89; $^3J_{Pt-H} = <10$
				2.89; $^3J_{Pt-H} = <10$
				2.86; $^3J_{Pt-H} \sim 33$
(tmeda)Pt(CH_2Ph)Cl (**5**)	CD_2Cl_2 (300 MHz)	25	Pt-C***H***$_2$Ph	2.96 (s); $^2J_{Pt-H} = 109.8$
			Pt-N-C***H***$_3$	2.76 (s); $^3J_{Pt-H} = 83$
				2.70 (s); $^3J_{Pt-H} = <10$
			Pt-N-C***H***$_2$−	2.47 (m) [second multiplet obscured by peaks at 2.76 and 2.70]
(tmeda)Pt(CH_2Ph)(H)Cl_2 (**6**)	CD_2Cl_2	−60	Pt-C***H***$_a$H$_b$Ph	4.8 (d); $^2J_{Pt-H} = 107$, $^2J_{Ha-Hb} = 10$
			Pt-CH$_a$***H***$_b$Ph	3.2 (d); $^2J_{Pt-H} = 92$
			Pt-***H***	−23.9 (s); $^1J_{Pt-H} = 1230$
			Pt-N-C***H***$_3$	3.0; $^3J_{Pt-H} \sim 32$
				2.9; $^3J_{Pt-H} = <10$
				2.8; $^3J_{Pt-H} = <10$
				2.7; $^3J_{Pt-H} \sim 56$
(tmeda)Pt(CH_2Ph)$_2$ (**7**)	CD_2Cl_2	25	Pt-C***H***$_2$Ph	2.71 (s), $^2J_{Pt-H} = 122$
			Pt-N-C***H***$_3$	2.56 (s); $^3J_{Pt-H} = 20$
			Pt-N-C***H***$_2$−	2.54 (s); $^3J_{Pt-H} = <10$
(tmeda)Pt(CH_2Ph)$_2$(H)Cl (**8**)	CD_2Cl_2/Et_2O-d_{10} (10:1)	−20	Pt-C***H***$_a$H$_b$Ph	3.44 (d); $^2J_{Pt-H} = 95$, $^2J_{Ha-Hb} = 10$
			Pt-CH$_a$***H***$_b$Ph	3.31 (d); $^2J_{Pt-H} = 117$
			Pt-***H***	−23.1 (s); $^1J_{Pt-H} = 1630$
			Pt-N-C***H***$_3$	2.76 (s), $^3J_{Pt-H} = <15$
				2.51 (s), $^3J_{Pt-H} = 27$
			Pt-N-C***H***$_2$−	2.63 (br s)
				2.91 (br s)
(4,4′-Me_2-2,2′-bpy_2)Pt(CH_3)$_2$ (**9**)	CD_2Cl_2	25	Pt-C***H***$_3$	0.90 (s); $^2J_{Pt-H} = 85$
			Pt-(py-C***H***$_3$)	2.36 (s)
(4,4′-Me_2-2,2′-bpy_2)Pt(CH_3)$_2$(H)Cl (**10**)	CD_2Cl_2/Et_2O-d_{10} (10:1)	−65	Pt-C***H***$_3$	1.25 (s); $^2J_{Pt-H} = 66$
			Pt-***H***	−22.1 (s); $^1J_{Pt-H} = 1610$
			Pt-(py-C***H***$_3$)	2.44 (s)
(tmeda)Pt(CH_3)$_2$(H)Cl (**12**)	CD_3OD	−50	Pt-C***H***$_3$	0.87 (s, 3 H); $^2J_{Pt-H} = 66$
			Pt-***H***	-23.1(s); $^1J_{Pt-H} = 1726$
			Pt-N-C***H***$_3$	2.78 (s); $^3J_{Pt-H} = 24$
				2.72 (s); $^3J_{Pt-H} = 10$
			Pt-N-C***H***$_2$−	2.91 (br s)
[(tmeda)Pt(CH_3)$_2$(H)(CD_3OH)](OTf) (**13**)	CD_3OD	−55	Pt-C***H***$_3$	0.84 (s); $^2J_{Pt-H} = 66$
			Pt-***H***	−23.1 (s); $^1J_{Pt-H} = 1721$
			Pt-N-C***H***$_3$	2.79 (s); $^3J_{Pt-H} = 27$
				2.70 (s); $^3J_{Pt-H} = <10$
			Pt-N-C***H***$_2$−	2.91 (br s)
trans-(PEt_3)$_2$Pt(CH_3)Cl (**15**)	$CDCl_3$	25	Pt-C***H***$_3$	0.325 (t); $^3J_{P-H} = 6$; $^2J_{Pt-H} = 84$
(PEt_3)$_2$Pt(CH_3)(H)Cl_2 (**16**)	CD_2Cl_2/Et_2O-d_{10} (10:1)	−65	Pt-C***H***$_3$	0.935 (t); $^3J_{P-H} = 5$; $^2J_{Pt-H} = 65$
			Pt-***H***	−18.8 (t); $^2J_{P-H} = 6$; $^1J_{Pt-H} = 1223$

effect, (K_H/K_D) = 0.51 ± 0.05 (−28 °C), for equilibrium 5.

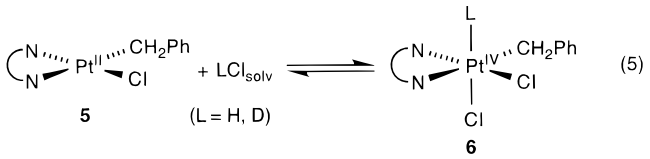

5 6 (5)

Comparison of the resulting concentrations of $PhCH_3$ versus $PhCH_2D$ generated upon decomposition of this mixture of isotopomers indicates a kinetic deuterium isotope effect for reductive elimination $k_H/k_D = 1.55 \pm 0.10$ at both −28 and 0 °C.

Protonolysis of (tmeda)Pt(CH_2Ph)$_2$, (4,4′-Dimethyl-2,2′-bipyridyl)Pt(CH_3)$_2$, and (tmeda)Pt(CH_3)$_2$ in Methylene Chloride. Since the Pt(IV) complexes described above were not characterized by X-ray crystallography, we were unable to unambiguously establish the stereochemistry of HCl addition to **2** or **5**. We gained further insight by investigating the reaction of HCl with dialkylplatinum(II) species, since the products exhibit greater symmetry. Protonation of (tmeda)Pt(CH_2Ph)$_2$ (**7**) produces (tmeda)Pt(CH_2Ph)$_2$(H)Cl (**8**) which exhibits two inequivalent resonances for its tmeda methyl protons in the ^{1}H NMR spectrum at −45 °C (Table 1). Furthermore, addition of HCl to (4,4′-dimethyl-2,2′-bipyridyl)Pt(CH_3)$_2$ (**9**) leads to a dialkylhydridoplatinum(IV) complex (**10**) with only a single resonance in the ^{1}H NMR spectrum corresponding to the methyls on the bipyridyl ligand (see Table 1). These results indicate trans addition of HCl to **7** and **9**, and thus, by extension, to **2** and **5** as well (see Discussion section).

During this study, we discovered that dialkylhydridoplatinum(IV) complexes are more stable than the corresponding monoalkylhydridoplatinum(IV) species with respect to alkane loss. Whereas (tmeda)Pt(CH_2Ph)(H)Cl_2 (**6**) eliminates toluene at approximately −30 °C, a comparable rate for reductive elimination from (tmeda)Pt(CH_2Ph)$_2$(H)Cl (**8**) does not occur until −5

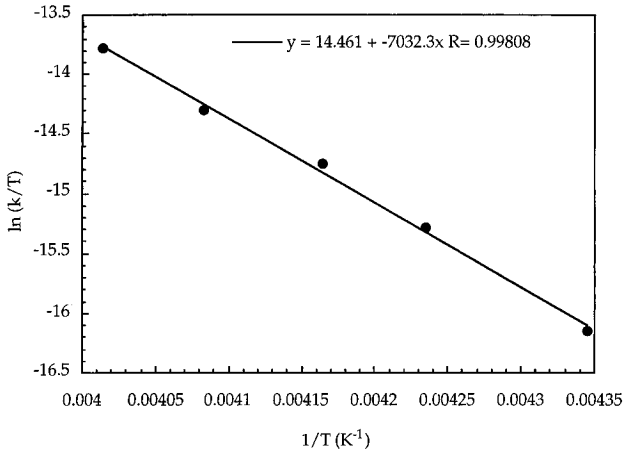

Figure 3. Eyring plot for the reductive elimination of toluene from **6** in CD_2Cl_2. Calculated activation parameters: $\Delta H^{\ddagger} = -14.0 \pm 2.5$ kcal/mol, $\Delta S^{\ddagger} = -18.5 \pm 7.0$ eu. [**6**] = 13 mM; [HCl] = 65 mM; temperature = −24 to −43 °C.

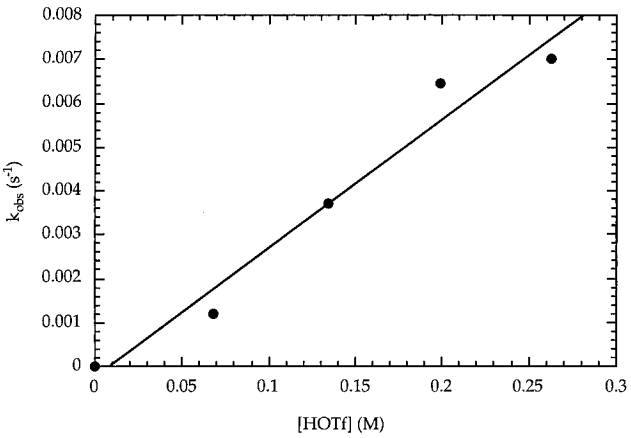

Figure 4. [HOTf] dependence of the rate of reductive elimination of toluene from **5** in CD_2Cl_2. [HOTf] = 0−20 equiv (relative to [**6**]); [**6**] = 13 mM; [HCl] = 65 mM; temperature = −61 °C.

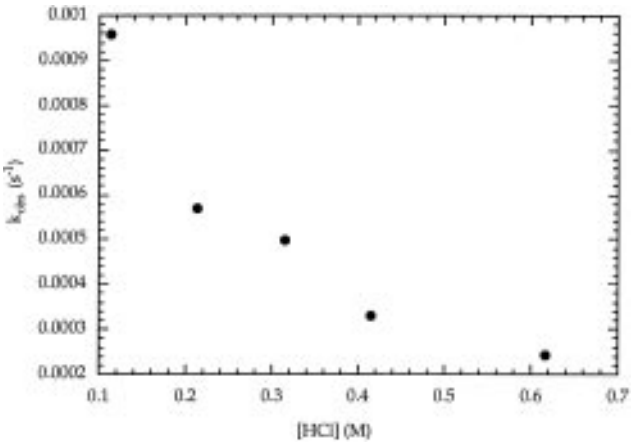

Figure 5. Plot of k_{obs} versus [HCl] revealing that HCl inhibits the reductive elimination of toluene from **6** in CD_2Cl_2 when [HOTf] is present. [HCl] = 9.4−51 equiv (relative to [**6**]); [**6**] = 12 mM; [HOTf] = 61 mM; temperature = −62 °C.

°C. The methyl derivatives (tmeda)Pt(CH_3)(H)Cl_2 (**4**) and (tmeda)Pt(CH_3)$_2$(H)Cl (**12**) show a more pronounced effect—methane loss from **4** occurs rapidly at −60 °C, but not until *+10* °C from **12**.

Protonolysis of (tmeda)Pt(CH_3)$_2$ (11) in CD_3OD. Upon observing the higher stability of dialkylhydridoplatinum(IV) species, we investigated the protonolysis of (tmeda)Pt(CH_3)$_2$ (**11**) in methanol. Since **11** appears to decompose in methanol

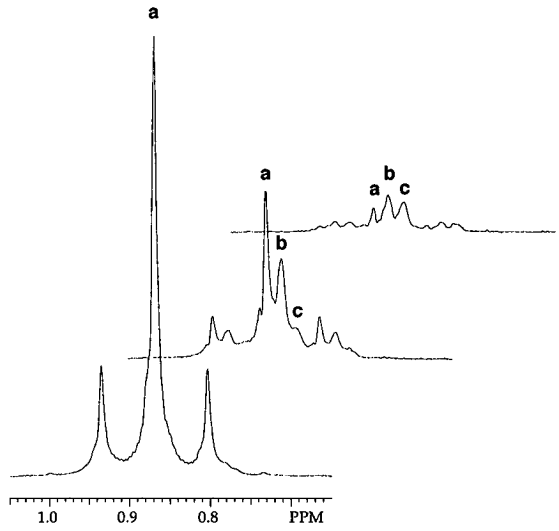

Figure 6. Sequence of ^{1}H NMR spectra demonstrating the appearance of shoulders upfield of the original Pt(IV)−CH_3 resonance from **12** in CD_3OD along with an overall decrease in the peak integration. The upfield shoulders are assigned as the sequentially deuterated methyl groups: **a** = Pt−CH_3, **b** = Pt−CH_2D, and **c** = Pt−CHD$_2$.

Scheme 3

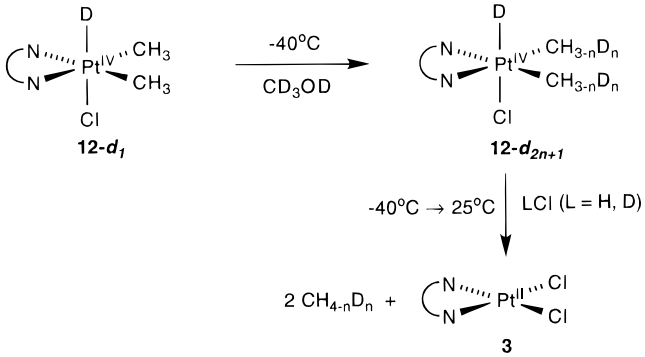

even in the absence of acid at room temperature,[40] the following procedure was adopted: **11** was dissolved in a minimal amount of CD_2Cl_2 and then cooled to −78 °C before adding methanol-d_3 (CD_3OH:CD_2Cl_2 = 13:1). Subsequent addition of excess HCl to this solution at −78 °C leads to formation of the oxidative addition product, (tmeda)Pt(CH_3)$_2$(H)Cl (**12**) (Table 1). Addition of HOTf also leads to a stable alkylhydridoplatinum(IV) complex, presumably the methanol coordinated product, [(tmeda)Pt(CH_3)$_2$(H)(CD_3OH)](OTf) (**13**) (Table 1). Significantly, monitoring the ^{1}H NMR spectrum of **12-d_1** in CD_3OD as it is warmed to −40° C revealed deuterium incorporation into the methyl positions (Scheme 3, Figure 6). When warmed to room temperature to allow methane loss prior to complete deuterium exchange, the full range of methane isotopomers is observed (Figure 7).

H/D exchange rates were obtained by monitoring the decrease in total integration of ^{1}H NMR signals corresponding to Pt−CL_3 (L = H, D) for a solution of **12** in CD_3OD. The activation parameters for H/D exchange were derived from an Eyring plot: $\Delta H^{\ddagger} = 15.8$ (±1.8) kcal/mol and $\Delta S^{\ddagger} = -4.7$ (±7.5) eu.[41] At constant ionic strength, added chloride inhibits H/D

(40) No methane is generated in this side reaction. The reactivity is likely related to that previously observed for similar compounds dissolved in protic solvents (alcohols and water): (a) Monaghan, P. K.; Puddephatt, R. J. *Organometallics* **1984**, *3*, 444. (b) Holtcamp, M. W.; Labinger, J. A.; Bercaw, J. E. Unpublished results.

(41) Reaction conditions (Eyring plot for deuterium incorporation into **12** in CD_3OD:CD_2Cl_2 (13:1)): [**12**] = 21 mM; [H^+] = 0.21 M; [Cl^-] = 0.20 M; μ = 1.21 M; temperature range −31 to −55 °C.

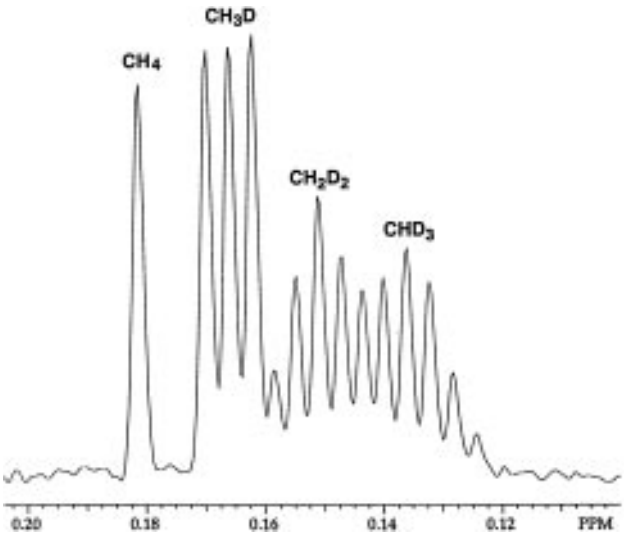

Figure 7. Full range of methane isotopomers that arise upon warming a reaction mixture containing **12** in CD_3OD prior to complete deuterium incorporation into the platinum−methyl groups.

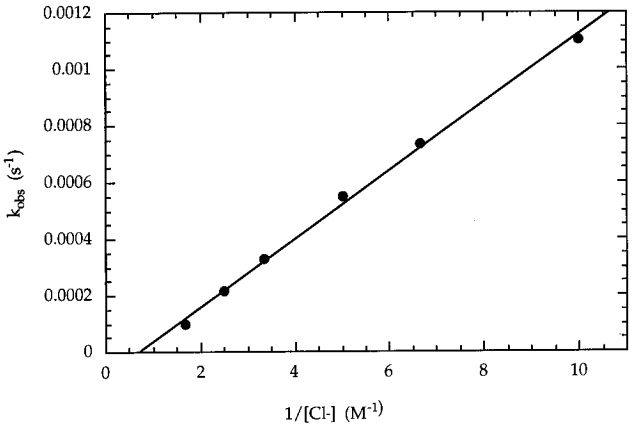

Figure 8. Plot of k_{obs} versus 1/[Cl^-] for deuterium incorporation into **12** in CD_3OD:CD_2Cl_2 (13:1). [Cl^-] = 0.10−0.60 M; [**12**] = 21 mM; [H^+] = 0.21 M; μ = 1.21 M; temperature = −43 °C.

exchange, and the rate was found to depend on the inverse of [Cl^-] (see Figure 8).

By monitoring the ^{1}H NMR resonance of methylplatinum(IV) in CD_3OH (*i.e.*, a solvent in which no H/D exchange occurs), **12** was found to lose methane cleanly at approximately −25 °C exhibiting first-order kinetics with activation parameters: $\Delta H^{\ddagger}$ = 19.1 (±0.6) kcal/mol and $\Delta S^{\ddagger}$ = 4.1 (±2.2) eu.[42] The rate of methane elimination from **12** is also inversely proportional to the chloride concentration (Figure 9).

As expected, (tmeda)Pt(CH_3)Cl (**2**) is not observed during the conversion of **12** to **3**; **2** decomposes rapidly under these conditions (see above). However, a different methylplatinum(II) intermediate (**14**) does appear as the reaction proceeds. The amount of **14** observed in solution decreases as the initial chloride concentration is increased; furthermore, loss of methane from **14** does not take place until approximately +15 °C—well above the temperature for methane loss from **12** or **2**. **14** was identified as [(tmeda)Pt(CH_3)(methanol)]$^+$ by independent synthesis (from treating **2** with AgOTf) and comparison of ^{1}H NMR parameters and protonolysis behavior. Fortunately, formation of **14** does not interfere with the kinetics for conversion of **12** to methane and **3**.

(42) Reaction conditions (Eyring plot for methane elimination from **12** in CD_3OH:CD_2Cl_2 (13:1)): [**12**] = 21 mM; [H^+] = 0.21 M; [Cl^-] = 0.20 M; μ = 1.21 M; temperature range −15 to −35 °C.

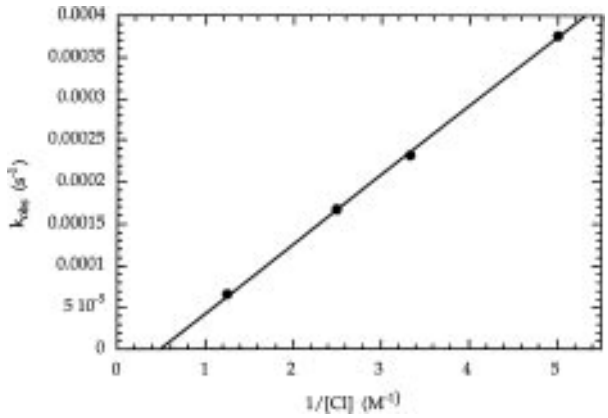

Figure 9. Plot of k_{obs} versus 1/[Cl^-] for methane elimination from **12** in CD_3OH:CD_2Cl_2 (13:1). [Cl^-] = 0−0.80 M; [**12**] = 21 mM; [H^+] = 0.21 M; μ = 1.21 M; temperature = −28 °C.

Proton incorporation into the platinum−methyl positions of (tmeda)Pt(CD_3)$_2$(H)Cl (**12-*d*$_6$**) in CH_3OH and CD_4 loss from **12-*d*$_7$** in CH_3OD were monitored by ^{2}D NMR. Kinetic isotope effects were calculated by comparing these rates with those for deuterium incorporation and CH_4 loss from **12**: k_H/k_D = 1.9 (±0.2) at −47.6 °C for H/D incorporation into Pt−CL_3; k_H/k_D = 0.29 (±0.05) at −26.8 °C for methane loss.

Protonolysis of *trans*-(PEt$_3$)$_2$Pt(CH_3)Cl (15) in Methylene Chloride and Methanol. Addition of HCl (as a Et_2O-d_{10} solution) to a CD_2Cl_2 solution of *trans*-(PEt$_3$)$_2$Pt(CH_3)Cl (**15**) at −78 °C generates (PEt$_3$)$_2$Pt(CH_3)(H)Cl_2 (**16**) (eq 6).

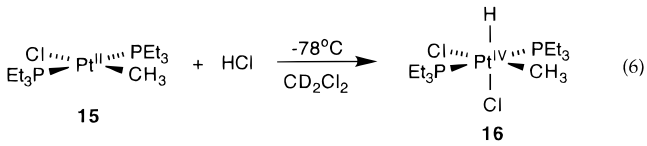

(6)

The ^{1}H NMR spectrum for **16** clearly reveals the hydride resonance at δ −18.8 ppm with coupling to both platinum and phosphorus (Table 1). Consistent with the formation of a platinum(IV) complex, the resonances associated with the methyl group shift downfield and the two-bond platinum−hydrogen coupling constant decreases relative to **15**. As the solution is warmed to approximately −45 °C loss of methane is observed along with formation of (PEt$_3$)$_2$$PtCl_2$ (**17**) (eq 7).

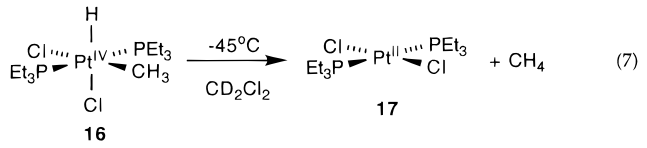

(7)

Protonolysis of **15** in CD_3OH revealed yet another reaction pattern. Addition of DOTf to **15** in CD_3OD at −78 °C (μ = 1 M) produces no reaction, *i.e.*, neither an alkylhydridoplatinum(IV) intermediate nor methane is generated. But as the solution is warmed to −25 °C, deuterium incorporation into the Pt−CH_3 sites takes place with *no* Pt(IV) intermediate observed (Scheme 4); only **15** and its isotopomers are detected in solution by ^{1}H NMR spectroscopy prior to methane loss. The kinetics were monitored by integrating the total Pt−$CH_{3-n}D_n$ ^{1}H NMR signal over time (Figure 10).

In the presence of DOTf, with no excess chloride added to the reaction mixture, full deuterium incorporation takes place with no competition from methane loss. As the chloride concentration is increased, methane loss begins to compete with H/D exchange. Rate data for the loss of methane from **15** were obtained by monitoring the protonolysis reaction in CD_3OH (i.e.,

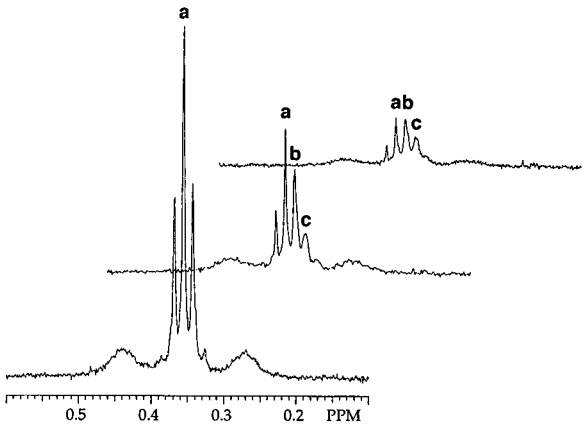

Figure 10. Sequence of ^{1}H NMR spectra demonstrating the appearance of new resonances upfield of the original $Pt^{II}-CH_3$ resonance from **15** along with an overall decrease in the peak integration. The upfield resonances are assigned as the sequentially deuterated methyl groups: **a** = Pt−CH_3, **b** = Pt−CH_2D, and **c** = Pt−CHD$_2$.

Scheme 4

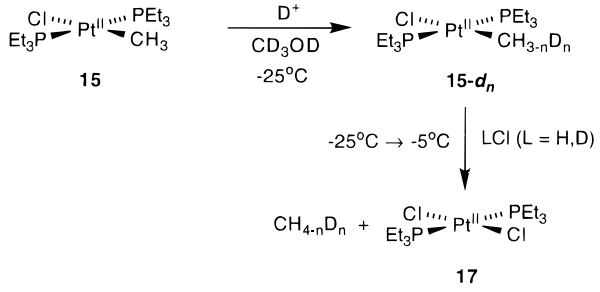

in the absence of H/D exchange) at −5 °C in the presence of 0.14 M chloride.[43]

The rate of H/D exchange exhibits a first-order dependence on [Cl$^-$] (Figure 11). Loss of methane from **15** in CD_3OH is also dependent on chloride concentration (approximately first order) (Figure 11). In contrast to the chloride dependence for H/D exchange, methane loss exhibits no measurable rate when [Cl$^-$] = 0 (Figure 11).

Activation parameters were determined for both reactions: for H/D exchange, $\Delta H^{\ddagger} = 14.5$ (±1.5) kcal/mol and $\Delta S^{\ddagger} = -14.8$ (±4.5) eu,[44] and for loss of methane, $\Delta H^{\ddagger} = 16.8$ (±0.8) kcal/mol and $\Delta S^{\ddagger} = -12.5$ (±2.6) eu.

Preparation of *trans*-$(PEt_3)_2Pt(CD_3)Cl$ (**15-d_3**) allowed the determination of kinetic isotope effects for both H/D exchange and loss of methane. Both isotope effects obtained for this system are *inverse*: $k_H/k_D = 0.80$ (±0.05) at −26.8 °C for H/D exchange, and $k_H/k_D = 0.11$ (±0.02) at −12.0 °C for methane loss.

Reduction of $[Pt^{IV}MeCl_5]^{2-}$ in Methanol-$d_{3,4}$ and Water-$d_{0,2}$. Reduction of $[Pt^{IV}MeCl_5]^{2-}$ (**19**) with 2 equiv of $CrCl_2$ in a 10:1 mixture of D_2O:H_2O at 0 °C generates CH_4 and CH_3D (3.2:3.6), from which a kinetic deuterium isotope effect is calculated: $k_H/k_D = 8.8$ (±0.5). Upon warming a heterogeneous mixture of $[Pt^{IV}MeCl_5]^{2-}$ and $CrCl_2$ in CD_3OD:CD_3OH (4:1) from −78 to 0 °C, the reagents dissolve and methane evolution is observed. The methane generated is composed of a mixture of CH_4, CH_3D, and CH_2D_2 (∼2.6:2.2:1).[45]

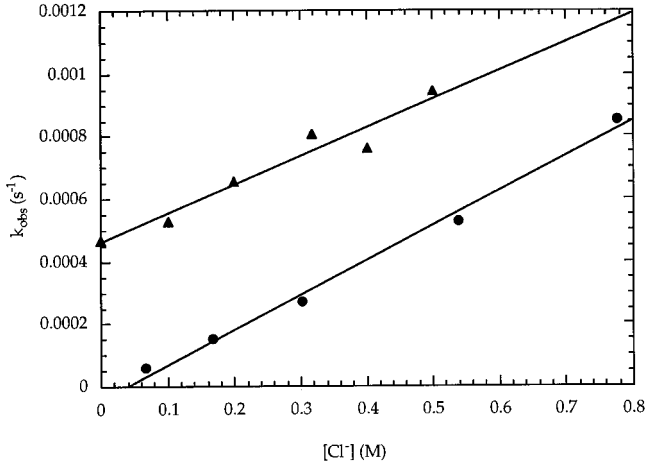

Figure 11. Plot of k_{obs} versus [Cl$^-$] for deuterium incorporation into **15** in CD_3OD (Δ) and for the protonolysis of **15** in CD_3OH (●). Conditions for H/D exchange: [Cl$^-$] = 0.10−0.50 M; [**15**] = 15 mM; [H$^+$] = 0.15 M; μ = 1.15 M; temperature = −23 °C. Conditions for protonolysis: [Cl$^-$] = 0.067−0.78 M; [**15**] = 15 mM; [H$^+$] = 0.15 M; μ = 1.15 M; temperature = −10 °C.

Discussion

Relevance of Model Complexes. Based on the principle of microscopic reversibility, a mechanistic study of the protonolysis of alkylplatinum(II) could provide insight into C−H activation by Pt(II). Although we had originally hoped to conduct our mechanistic studies on the catalytic intermediate $[Cl_3Pt^{II}CH_3]^{2-}$ (**1**), we encountered a series of complications while studying this species (see Introduction).[12,26] We therefore chose to investigate the protonolysis of (tmeda)Pt(CH_3)Cl (**2**). The relevance of this model is supported by the ability of tmeda-ligated platinum species to undergo reactions directly analogous to those proposed for catalytic alkane oxidation (steps I, II, and III in Scheme 5).[12] Further support derives from the observation of isotopic exchange prior to liberation of methane when **1** is generated by reduction of **19** in CD_3OD, behavior closely resembling that of several of the model systems. Nevertheless, whenever one investigates model chemistry, there always exists a certain degree of ambiguity with respect to its relevance to the "real" system.

Protonolysis of (tmeda)Pt(CH_3)Cl (2) in CD_3OD. Although the protonolysis of alkylplatinum(II) species has been investigated previously by a variety of other groups, no consensus has been reached on the detailed mechanism of the reaction. Only indirect evidence such as kinetic analysis, isotope effects, and competition experiments was available in these studies until recently. Protonolysis of **2** in CD_3OD is no exception.

This reaction's first-order dependence on chloride and proton concentration (Figures 1 and 2) combined with the non-zero intercept in Figure 2 supports a two-term rate law (eq 8), namely

$$\text{rate} = k_2[\mathbf{2}][H^+] + k_3[\mathbf{2}][H^+][Cl^-] \qquad (8)$$

one term independent of [Cl$^-$] and the other with a first-order

(43) In the absence of added chloride ([Cl$^-$] < 0.14 M), side reactions complicate the kinetics. Upon methane loss from **15**, the product $(PEt_3)_2$-Pt(Cl)(OTf) can abstract chloride from **15** to generate a new phosphine-ligated methylplatinum(II) species, $(PEt_3)_2Pt(CH_3)(OTf)$ (**18**), which is much less reactive toward protonolysis. Small amounts of **18** can be identified in these reaction mixtures by ^{1}H NMR spectroscopy, and the spectroscopic data are consistent with independently prepared samples of **18**. These results will be discussed in further detail in a future paper: Holtcamp, M. W.; Labinger, J. A.; Bercaw, J. E. Unpublished results.

(44) Reaction conditions (Eyring plot for deuterium incorporation into **15** in CD_3OD): [**15**] = 15 mM; [H$^+$] = 0.15 M; [Cl$^-$] = 0.14 M; μ = 1.15 M; temperature range −13 to −40 °C.

(45) Along with formation of methane, another methylplatinum species is produced in the reaction mixture as observed by ^{1}H NMR spectroscopy. This product appears consistent with $[PtMe_2Cl_4]^{2-}$, formed by nucleophilic attack by Pt(II) (from $[PtMeCl_3]^{2-}$, **1**) at carbon in $[PtMeCl_5]^{2-}$ displacing $[PtCl_4]^{2-}$ (see ref 26). This reaction competes with the protonolysis of **1**.

Scheme 5

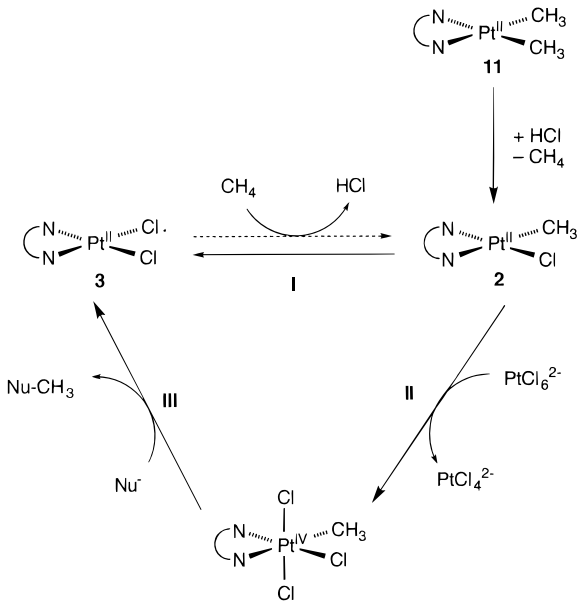

dependence on [Cl^-]. Various rate laws have been obtained in related studies, and that shown in eq 8 is not without precedent. This rate law can be interpreted in several different ways, however. Initially, this rate law was invoked to support the intermediacy of an alkylhydridoplatinum(IV) species (intermediate **A**) which subsequently reductively eliminates alkane.[27] According to this mechanism, the chloride-dependent term in the rate law reflects stabilization of the Pt(IV) intermediate by chloride coordination. The chloride-independent term, then, implies a parallel, solvent-stabilized version of intermediate **A** (which is kinetically invisible).

It has been recognized, however, that this rate law is also consistent with chloride-assisted, direct electrophilic attack at the Pt−C bond (transition states **B** or **C**).[28] The four-centered "σ-bond metathesis"-style mechanism (**B**) has been commonly invoked in electrophilic attack of alkylmercury(II) and other species which do not have an accessible higher oxidation state,[46−48] and a recent theoretical study has analyzed this pathway for C−H activation by platinum(II).[31] Transition state **C** was proposed by Alibrandi *et al.* following an extensive kinetic study of alkylplatinum(II) species.[28]

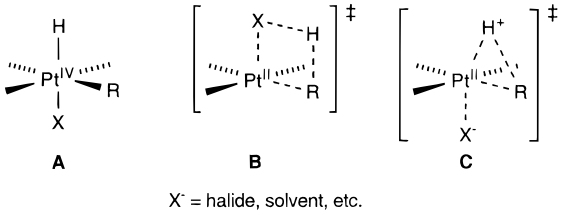

With respect to the activation of alkanes to generate the alkylplatinum(II) intermediate, structure **A** reflects a mechanism involving alkane oxidative addition/alkylhydridoplatinum(IV) deprotonation (eq 1), whereas **B** and **C** are transition states along reaction profiles for non-redox processes as in the alternative (eq 2).

The activation parameters are of little value for mechanistic interpretation because of the significant role of ion solvation/desolvation in the entropy of activation. The isotope effects are also ambiguous. Isotope effects obtained from a competition experiment in protic solvents are well-known to be strongly affected by fractionation factors.[49,50] This consideration accounts for the discrepancy between the isotope effects obtained under competitive (i.e., comparing the ratio of methane isotopomers generated in a mixture of CD_3OH and CD_3OD—k_H/k_D = 9.1) versus non-competitive conditions (i.e., comparing the ratio of protonolysis rate constants measured for the two separate solvents—k_H/k_D = 2.3). Due in part to this complication, these values do not distinguish between the possible mechanisms.

Protonolysis of Alkylplatinum(II) Species in CD_2Cl_2. Simply changing the reaction solvent from CD_3OD to CD_2Cl_2 led to an important result: the identification of an alkylhydridoplatinum(IV) complex when tmeda was incorporated as a stabilizing ligand. Such intermediates had not been observed in alkylplatinum(II) protonolysis studies when we began our work. Since then, two other groups have identified similar species by hydrolyzing trialkylsilyl halides (to generate HX *in situ*; X = Cl, Br, I) in solutions of dialkylplatinum(II) complexes at low temperature. These reports also involved nitrogen-donor ligands (bipyridyl or phenanthroline ligands) to stabilize the platinum(IV) species. HCl addition to *trans*-$(PEt_3)_2Pt(CH_3)Cl$ (**15**) (i.e., a complex containing soft ligands) in CD_2Cl_2 (eq 6) also yields the platinum(IV) product at low temperature. These observations appear to refute earlier proposals, based on an extensive study of phosphine-ligated complexes (including **15**), that protonolysis of alkylplatinum(II) always proceeds via a concerted mechanism (specifically, transition state **C**).[28]

We next considered the detailed mechanism of alkane reductive elimination. Nearly all of our mechanistic work focused on loss of toluene from (tmeda)$Pt(CH_2Ph)(H)Cl_2$ (**6**). It was straightforward to demonstrate that oxidative addition of HCl to alkylplatinum(II) was rapid and reversible on the time scale of hydrocarbon elimination. The negative entropy of activation ($\Delta S^{\ddagger} = -18.5 \pm 7.0$ eu) obtained for this reaction suggests a mechanism other than simple reductive elimination from 6-coordinate Pt(IV). Reductive elimination reactions often exhibit near-zero or positive entropies of activation due to the formation of two products from one reactant. Formation of an ionic intermediate can lead to a negative entropy of activation due to significant ordering of the solvent molecules;[51] in our system, chloride dissociation could lead to such an intermediate. Our first attempt to verify such a mechanism by checking for chloride inhibition was thwarted, however, because excess chloride deprotonates **6** to regenerate **5** (eq 4). We did obtain support for this mechanism by adding HOTf or $SnCl_4$ to a solution of **6**; addition of either reagent greatly accelerates the rate of toluene elimination.

A possible mechanism for the reductive elimination of toluene from **6** in the presence of HOTf is shown in Scheme 6. This mechanism suggests that chloride must dissociate from **6** to generate a five-coordinate cationic intermediate **20** prior to reductive elimination. Triflic acid facilitates loss of chloride; Lewis acids such as $SnCl_4$ function similarly. Prerequisite ligand dissociation has been identified in previous studies of alkyl hydride reductive elimination,[52−54] although this mechanistic feature is by no means universal.[55−58]

(46) Abraham, M. H. *Mechanisms of Electrophilic Substitution at Saturated Carbon*; Amsterdam, 1973.
(47) Kochi, J. K. *Organometallic Mechanisms and Catalysis*; Academic Press: New York, 1978; pp 292−340.
(48) Nugent, W. A.; Kochi, J. K. *J. Am. Chem. Soc.* **1976**, *98*, 5979.
(49) Bell, R. P. *The Proton in Chemistry*; Cornell University Press: Ithaca, NY, 1973.
(50) Melander, L.; Saunders, W. H. *Reaction Rates of Isotopic Molecules*; Krieger: Malabar, FL, 1987; p 202.
(51) A very large negative entropy of activation (−39 ± 4 eu) has been obtained for ethane elimination from dimethylpalladium(IV) in which iodide dissociation has been shown to precede alkane loss: Byers, P. K.; Canty, A. J.; Crespo, M.; Puddephatt, R. J.; Scott, J. D. *Organometallics* **1988**, *7*, 1363.
(52) Milstein, D. *J. Am. Chem. Soc.* **1982**, *104*, 5227.

Scheme 6

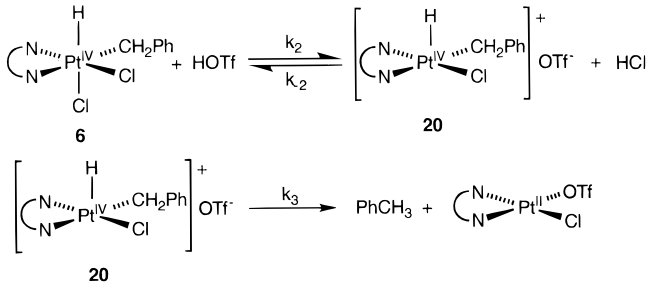

Scheme 7

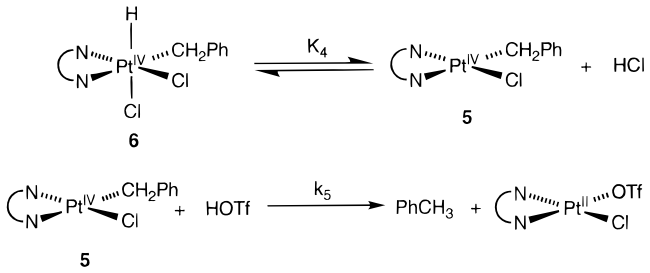

Table 2. Predicted Rate Expressions for Mechanisms Proposed in Schemes 6 and 7

	Scheme 6	Scheme 7
pre-equilibrium first step	k_3K_2[HOTf][**6**]/[HCl]	k_5K_4[HOTf][**6**]/[HCl]
steady state	k_2k_3[HOTf][**6**]/{$k_3 + k_{-2}$[HCl]}	k_4k_5[HOTf][**6**]/{k_{-4}[HCl] + k_5[HOTf]}

An alternative mechanism that might also be considered is shown in Scheme 7. Here **6** is merely generated in an unproductive side reaction, while alkane formation requires reductive elimination of HCl from **6** followed by direct electrophilic attack by H^+ at the platinum alkyl bond of **5**. Indeed, both schemes look very similar kinetically, and the derived rate expressions have been outlined in Table 2. Both pre-equilibrium and steady-state situations have been considered. Because full equilibration between **6** and **5** was demonstrated by isotopic labeling (Scheme 2), the "steady-state" option for Scheme 7 is eliminated. The other three mechanistic possibilities were distinguished kinetically by evaluating the effect of [HCl] on the reaction rate with [HOTf] held constant. As demonstrated in Figure 5, the reaction is inhibited by HCl. Figure 12 shows the same data, presented as $1/k_{obs}$ vs [HCl]. The non-zero intercept in this plot supports the mechanism in Scheme 6 with steady-state kinetic behavior. Both pre-equilibrium rate laws predict that a plot of $1/k_{obs}$ vs 1/[HCl] would go through the origin. According to this mechanism, the negative entropy of activation would likely arise from ion solvation effects.

Isotope effects determined for this system (using calibrated mixtures of HCl and DCl) also support the mechanism in Scheme 6. Based on the isotope effects that were determined in this system ($K_H/K_D = 0.51$ for pre-equilibrium oxidative addition of LCl to **5**, and $k_H/k_D = 1.55$ for overall toluene formation from **5** + LCl (L = H, D)), other isotope effects for Schemes 6 and 7 can be calculated. If Scheme 6 is the correct mechanism, a kinetic deuterium isotope effect for the reductive elimination of toluene from **6** is $k_H/k_D = 3.1$ (±0.6) ($KIE_{overall} = EIE_{HClox.addn.} \times KIE_{k_3}$). This value is similar to those observed in alkane reductive elimination of platinum(II) alkyl hydrides.[55,56,59] On the other hand, if Scheme 7 is the operating mechanism, the isotope effect for k_5 is simply the observed overall isotope effect, $k_H/k_D = 1.55$. This value appears rather low for a single-step mechanism involving direct proton transfer.[60] Therefore, based on the kinetic argument described above and these isotope effect calculations, we favor the mechanism proposed in Scheme 6.

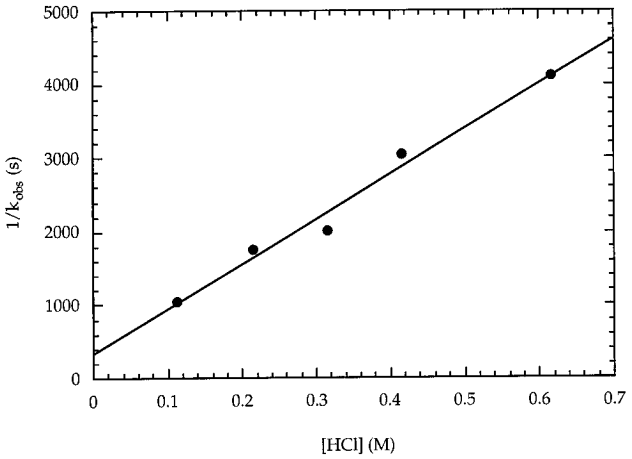

Figure 12. $1/k_{obs}$ vs [HCl] for reductive elimination of toluene from **6** in the presence of varying [HCl] and constant [HOTf]. For reaction conditions see Figure 5.

Stereochemistry of HCl Addition. The spectroscopic data obtained for **4** and **6** (Table 1) are unable to distinguish between *trans* versus *cis* addition of HCl to **2** and **5**, respectively. In theory, four possible stereoisomers could arise from this reaction (structures **D**−**G**). *Trans* addition of HCl would lead to

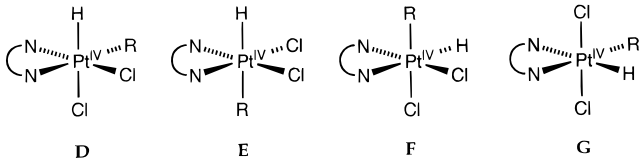

structure **D**, whereas *cis* addition could produce any of the structures **D**−**G**. Of course, any of the structures are also accessible via isomerization during or after the addition of HCl. Compound **6** contains four spectroscopically distinct methyl groups on the tmeda ligand (Table 1), consistent with structures **D** and **F**.

Evaluating HCl addition to related *dialkyl*platinum(II) species provided further insight. There are still four possible products however (structures **H**−**K**). In the absence of isomerization,

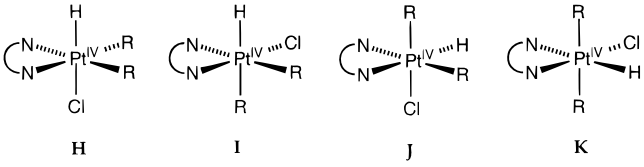

structure **H** results from *trans* addition of HCl, **I** and **J** from

(53) Basato, M.; Morandini, F.; Longato, B.; Bresadola, S. *Inorg. Chem.* **1984**, *23*, 649.
(54) Basato, M.; Morandini, F.; Bresadola, S. *Inorg. Chem.* **1984**, *23*, 3972.
(55) Abis, L.; Sen, A.; Halpern, J. *J. Am. Chem. Soc.* **1978**, *100*, 2915.
(56) Michelin, R. A.; Faglia, S.; Uguagliati, P. *Inorg. Chem.* **1983**, *22*, 1831.
(57) Buchanan, J. M.; Stryker, J. M.; Bergman, R. G. *J. Am. Chem. Soc.* **1986**, *108*, 1537.
(58) Jones, W. D.; Feher, F. J. *Acc. Chem. Res.* **1989**, *22*, 91.
(59) Hackett, M.; Ibers, J. A.; Whitesides, G. M. *J. Am. Chem. Soc.* **1988**, *110*, 1436.
(60) Moore, J. W.; Pearson, R. G. *Kinetics and Mechanism*, 3rd ed.; John Wiley & Sons: New York, 1981; p 367.

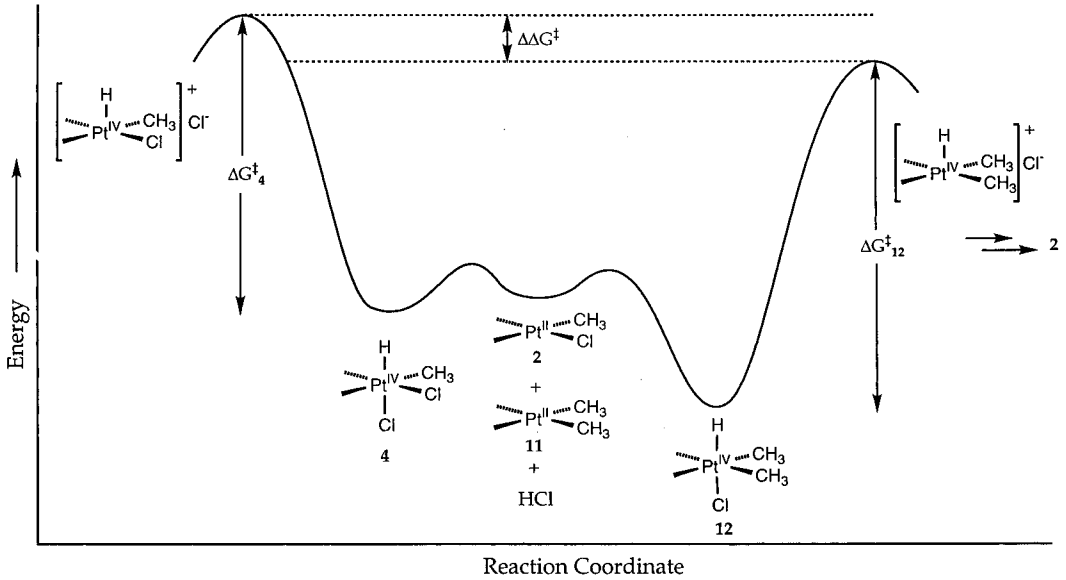

Figure 13. Qualitative reaction coordinate diagram for the reaction of HCl with **2** and **11**. While the barrier to reductive elimination from **12** ($\Delta G_{12}^{\ddagger}$) is greater than from **4** ($\Delta G_4^{\ddagger}$), the overall barrier to the reaction of HCl with **11** is lower than with **2** ($\Delta\Delta G^{\ddagger}$).

cis addition. The remaining stereoisomer, **K**, can only arise from isomerization following HCl addition. The ^{1}H NMR spectrum of (tmeda)Pt(CH_2Ph)$_2$(H)Cl (**7**) exhibits two inequivalent resonances for its tmeda methyl protons (Table 1). This spectrum is consistent with either structure **H** or **K**. Protonation of (4,4′-dimethyl-2,2′-bipyridyl)Pt(CH_3)$_2$ (**9**) leads to a dialkylhydridoplatinum(IV) complex (**10**) with only a single resonance in the ^{1}H NMR spectrum corresponding to the methyls on the bipyridyl ligand (Table 1). This result is only consistent with the *trans* HCl addition product **H**, a conclusion also reached by Puddephatt and co-workers in an identical reaction between HCl and (4,4′-di-*tert*-butyl-2,2′-bipyridyl)Pt(CH_3)$_2$.[33] By contrast, Panunzi and co-workers have identified structure **J** as the product arising from HX (X = Cl, Br) addition to (dmphen)Pt(CH_3)$_2$ (dmphen = 2,9-dimethyl-1,10-phenanthroline) in acetone/diethyl ether solution.[32] As noted by both groups, this product geometry is likely due to the steric constraints of the dmphen ligand used in this reation. Nevertheless, by analogy to the products of HCl addition to dialkylplatinum(II) species, **7** and **9**, we believe the addition proceeds with *trans* stereochemistry. The spectroscopic data for (PEt_3)$_2$Pt(CH_3)(H)Cl$_2$ (**16**) are also consistent with *trans* HCl addition to **15**, although this has not been verified by experiments with related dialkyl complexes.

Stability of Dialkylhydridoplatinum(IV) versus Monoalkylhydridoplatinum(IV): A Digressionary Anomaly. We have previously reported that preparation of (tmeda)Pt(CH_3)Cl (**2**) is readily accomplished in high yield by addition of 1 equiv of HCl to (tmeda)Pt(CH_3)$_2$ (**11**) in CH_2Cl_2 (Scheme 5). Based on the decreased stability of (tmeda)Pt(CH_3)(H)Cl$_2$ (**4**) relative to (tmeda)Pt(CH_3)$_2$(H)Cl (**12**), we might have expected that once **2** begins forming in solution, it would be consumed more rapidly than **11**, leaving a 1:1 mixture of **11** and (tmeda)PtCl_2. Because mixing equal amounts of **11** and (tmeda)PtCl_2 in CD_2Cl_2 revealed only a minor amount of comproportionation after 24 h,[53] this is not a kinetically competent mechanism to account for the clean formation of **2** under preparative conditions.

This apparently anomalous result is perhaps best explained by the energy diagram in Figure 13. We demonstrated above that protonation of the alkylplatinum(II) complexes is rapid and reversible. In other words, a mixture containing (tmeda)Pt(CH_3)Cl, (tmeda)Pt(CH_3)$_2$, and HCl in CH_2Cl_2 will rapidly equilibrate between both alkylhydridoplatinum(IV) species, (tmeda)Pt(CH_3)(H)Cl$_2$ (**4**) and (tmeda)Pt(CH_3)$_2$(H)Cl (**12**), prior to reductive elimination. The relative stabilities of **4** and **12** with respect to reductive elimination indicate that $\Delta G_{12}^{\ddagger} > \Delta G_4^{\ddagger}$. However as long as the transition state for reductive elimination from **12** is lower in energy than the transition state for elimination from **4**, the reaction will selectively generate (tmeda)Pt(CH_3)Cl until either HCl or (tmeda)Pt(CH_3)$_2$ is consumed.

Protonolysis of (tmeda)Pt(CH_3)$_2$ (11) in CD_3OD. Because the protonolysis of (tmeda)Pt(CH_3)Cl (**2**) in methanol reveals no intermediate prior to loss of methane, whereas an alkylhydridoplatinum(IV) intermediate is observed in CD_2Cl_2, we must consider whether changing the solvent changes the protonolysis mechanism. However, observation of the dialkylhydridoplatinum(IV) species (tmeda)Pt(CH_3)$_2$(H)Cl (**12**) upon treating (tmeda)Pt(CH_3)$_2$ (**11**) with HCl in methanol verifies the viability of Pt(IV) intermediates in polar/protic solvent. Not only is a platinum(IV) intermediate observed, but deuterium from CD_3OD is incorporated into the platinum-bound methyl groups prior to reductive elimination of methane, implicating the potential involvement of an alkane σ-complex.

We propose the mechanism shown in Scheme 8 for protonolysis of **11** in methanol. The fundamental steps involve (1) pre-equilibrium oxidative addition of HCl to generate **12**, (2) dissociation of chloride to produce a cationic, five-coordinate intermediate (**21**), (3) reductive C−H bond formation leading to the Pt(II) methane σ-complex (**22**) (the nature of this interaction will be discussed below), and finally, (4) unimolecular dissociation of alkane resulting in the cationic methylplatinum(II) species (**14**). Trapping of **14** by chloride to form **2** results in the immediate liberation of the second equivalent of methane. (**2** has already been shown to be unstable under these reaction conditions.) Small to significant concentrations of **14** can be observed by ^{1}H NMR, depending on the initial chloride concentration.

According to this proposal, methane dissociation is the rate determining step; all preceding steps can fully equilibrate prior to loss of methane. In order for H/D exchange to take place, the σ-complex (**22**) must rearrange to coordinate a different C−H(D) bond prior to reversion to **21**.

Recently, significant evidence has been provided for alkane σ-complexes mediating the solution-phase reductive elimination and oxidative addition of alkanes at transition metal centers.[61−73]

Scheme 8

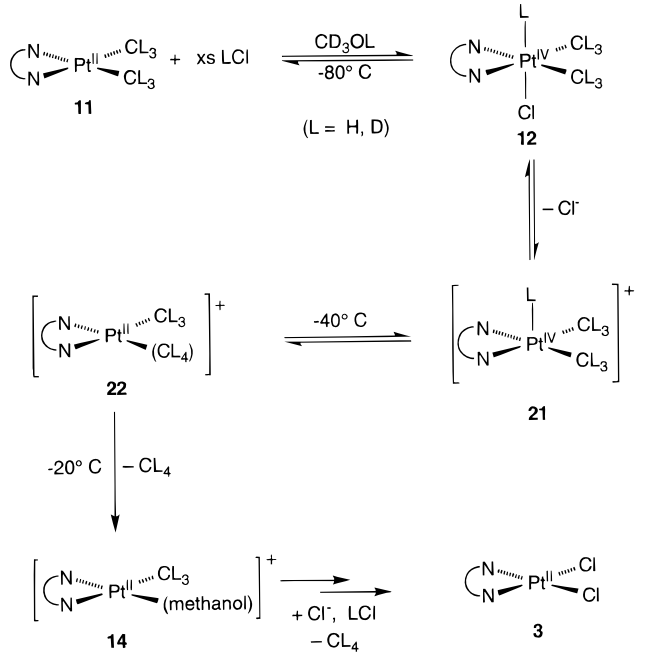

For example, Bergman, Moore, and co-workers have obtained transient IR spectroscopic data directly supporting such an intermediate in the oxidative addition of alkanes at a Cp*Rh(CO) fragment.[61−63] The viability of alkane adducts has received additional support from a variety of other sources: theory[74−78] and gas phase,[79−84] condensed phase,[85−89] and low-temperature matrix studies.[90,91] Furthermore, analogous η^2-dihydrogen and silane complexes along with 3-center-2-electron agostic C−H−M interactions[92] are now well-known and many have been structurally characterized.

Deuterium scrambling between hydride and alkyl positions prior to alkane elimination has been observed previously in other transition metal complexes.[64,65,67−73] In some cases the exchange proceeds rapidly enough to allow full equilibration of a single deuterium atom between the two different sites prior to methane loss. Equilibrium isotope effects determined in such cases reveal a preference for deuterium to reside in the alkyl site, as expected.[65,67,69,71] In our case, such equilibration leads to complete isotopic exchange because the platinum hydride also exchanges with the large excess of deuterium in the solvent. Complete proton incorporation into **12-*d*$_6$** is also observed when the reaction is carried out in CD_3OH. That H/D exchange takes place *intra*molecularly was verified by monitoring deuterium incorporation into **12** under approximately 15 atm of CH_4. No evidence for incorporation of CH_4 was obtained; loss of CL_4 in Scheme 8 is irreversible.

Although such isotopic exchange has been invoked to support the intermediacy of σ-complexes in the reductive elimination of alkanes, it is often difficult to definitively exclude alternative mechanistic possibilities. Such is the case here, too. The mechanism for H/D exchange need not lie on the reaction coordinate for reductive elimination. For example, it might proceed by formation of a carbene intermediate generated via α elimination or via deprotonation by an external base (e.g., solvent) (eqs 9 and 10, respectively). Reversal of either reaction could account for H/D exchange: in the former case, exchange of either platinum hydride with solvent deuterons followed by carbene insertion, or in the later case, deuteration of the platinum carbene by solvent deuterons.

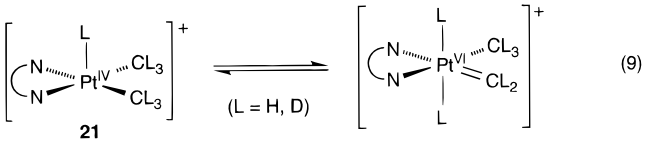

(9)

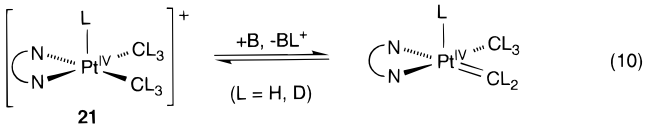

(10)

The magnitude of the normal isotope effect that we obtained for H/D exchange (k_H/k_D = 1.9 (±0.2)) appears unable to accommodate either carbene mechanism which should lead to *inverse* isotope effects. (The predicted inverse nature of these isotope effects arises solely from our definition of k_H and k_D. Both eqs 9 and 10 for H/D exchange involving a carbene intermediate should lead to faster rates for deuterium incorporation into $-CH_3$ (k_D) versus proton incorporation into $-CD_3$ (k_H).)

The inverse dependence of the rates of H/D exchange *and* methane elimination on chloride concentration (Figures 8 and 9) implies that chloride must dissociate from **12** prior to further reaction. A similar observation (involving iodide disso-

(61) Schultz, R. H.; Bengali, A. A.; Tauber, M. J.; Weiller, B. H.; Wasserman, E. P.; Kyle, K. R.; Moore, C. B.; Bergman, R. G. *J. Am. Chem. Soc.* **1994**, *116*, 7369.
(62) Bengali, A. A.; Schultz, R. H.; Moore, C. B.; Bergman, R. G. *J. Am. Chem. Soc.* **1994**, *116*, 9585.
(63) Bengali, A. A.; Arndtsen, B. A.; Burger, P. M.; Schultz, R. H.; Weiller, B. H.; Kyle, K. R.; Moore, C. B.; Bergman, R. G. *Pure Appl. Chem.* **1995**, *67*, 281.
(64) Buchanan, J. M.; Stryker, J. M.; Bergman, R. G. *J. Am. Chem. Soc.* **1986**, *108*, 1537.
(65) Periana, R. A.; Bergman, R. G. *J. Am. Chem. Soc.* **1986**, *108*, 7332.
(66) Jones, W. D.; Feher, F. J. *J. Am. Chem. Soc.* **1986**, *108*, 4814.
(67) Gould, G. L.; Heinekey, D. M. *J. Am. Chem. Soc.* **1989**, *111*, 5502.
(68) Bullock, R. M.; Headford, C. E. L.; Kegley, S. E.; Norton, J. R. *J. Am. Chem. Soc.* **1985**, *107*, 727.
(69) Bullock, R. M.; Headford, C. E. L.; Hennessy, K. M.; Kegley, S. E.; Norton, J. R. *J. Am. Chem. Soc.* **1989**, *111*, 3897.
(70) Parkin, G.; Bercaw, J. E. *Organometallics* **1989**, *8*, 1172.
(71) Wang, C.; Ziller, J. W.; Flood, T. C. *J. Am. Chem. Soc.* **1995**, *117*, 1647.
(72) Mobley, T. A.; Schade, C.; Bergman, R. G. *J. Am. Chem. Soc.* **1995**, *117*, 7822.
(73) Green, M. L. H. Personal communication.
(74) Cundari, T. R. *J. Am. Chem. Soc.* **1992**, *114*, 10557.
(75) Cundari, T. R. *J. Am. Chem. Soc.* **1994**, *116*, 340.
(76) Low, J. J.; Goddard, W. A. *Organometallics* **1986**, *5*, 609.
(77) Song, J.; Hall, M. B. *Organometallics* **1993**, *12*, 3118.
(78) Ziegler, T.; Tschinke, V.; Fan, L.; Becke, A. D. *J. Am. Chem. Soc.* **1989**, *111*, 9177.
(79) Brown, C. E.; Ishikawa, Y.; Hackett, P. A.; Rayner, D. M. *J. Am. Chem. Soc.* **1990**, *112*, 2530.
(80) Carroll, J. J.; Weisshaar, J. C. *J. Am. Chem. Soc.* **1993**, *115*, 800.
(81) Hop, C. E. C. A.; McMahon, T. B. *J. Am. Chem. Soc.* **1991**, *113*, 355.
(82) Ishikawa, Y.; Brown, C. E.; Hackett, P. A.; Rayner, D. M. *Chem. Phys. Lett.* **1988**, *150*, 506.
(83) Schroder, D.; Fiedler, A.; Hrusak, J.; Schwarz, H. *J. Am. Chem. Soc.* **1992**, *114*, 1215.
(84) Wasserman, E. P.; Moore, C. B.; Bergman, R. G. *Science* **1992**, *255*, 315.
(85) Dobson, G. R.; Hodges, P. M.; Healy, M. A.; Poliakoff, M.; Turner, J. J.; Firth, S.; Asali, K. J. *J. Am. Chem. Soc.* **1987**, *109*, 4218.
(86) Dobson, G. R.; Asali, K. J.; Cate, C. D.; Cate, C. W. *Inorg. Chem.* **1991**, *30*, 4471.
(87) Klassen, J. K.; Selke, M.; Sorensen, A. A. *J. Am. Chem. Soc.* **1990**, *112*, 1267.
(88) Simon, J. D.; Xie, X. *J. Phys. Chem.* **1989**, *93*, 291.
(89) Yang, C. K.; Peters, K. S.; Vaida, V. *Chem. Phys. Lett.* **1986**, *125*, 566.
(90) Billups, W. E.; Chang, S.-C.; Hauge, R. H.; Margrave, J. L. *J. Am. Chem. Soc.* **1993**, *115*, 2039.
(91) Perutz, R. N.; Turner, J. J. *J. Am. Chem. Soc.* **1975**, *97*, 4791.
(92) Crabtree, R. H. *Angew. Chem., Int. Ed. Engl.* **1993**, *32*, 789.

Scheme 9

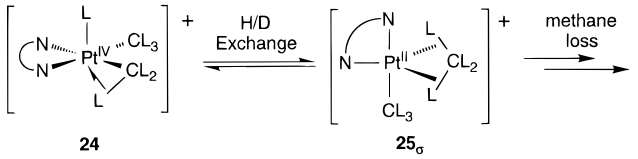

24 **25_σ**

ciation) has been made by Canty and Puddephatt *et al.* and Goldberg *et al.* when investigating the reductive elimination of ethane from trimethyl palladium(IV) and -platinum(IV) species, respectively.[51,93−96] Canty and Puddephatt suggest that upon iodide dissociation, an agostic interaction might develop between one of the methyl C−H bonds and the coordinatively unsaturated palladium center. This interaction could stabilize the redirection of a carbon sp^3 orbital away from the metal center and toward the second methyl group, ultimately leading to C−C bond formation. In our case, an agostic interaction could stabilize the *C−H* bond formation. The intermediate alkane σ-complex then might involve an η^3 (H−C−H) interaction with the metal center (**25_σ**) (Scheme 9). Such an alkane binding mode was evaluated in theoretical work by Low and Goddard as an intermediate in the reductive elimination of methane from Pt(II).[76] With such an intermediate, H/D exchange does not require that the bound alkane rearrange to coordinate a different C−H(D) bond as the oxidative C−H bond cleavage (**25_σ** → **24**) may select either coordinated bond. It should perhaps be noted that **25_σ** can be considered a resonance structure of a carbene complex (**25_c**). Unfortunately, we have no direct data that allow us to evaluate the nature of this intermediate further.

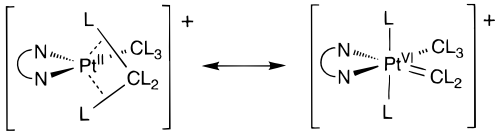

25_σ **25_c**

The isotope effect for methane loss from (tmeda)Pt$(CH_3)_2$(H)Cl (**12**) is substantially inverse (k_H/k_D = 0.29 (±0.05)). Inverse isotope effects have been reported by a number of groups who investigated the reductive elimination of alkanes from transition-metal centers; however, this is the smallest value obtained so far.[64,65,67,69−71] As has been discussed thoroughly in several of these references, inverse isotope effects often suggest the presence of an unobserved equilibrium preceding the rate-determining step. A single-step mechanism may also produce an inverse isotope effect;[97,98] however, one would expect such a value to arise only from a highly endothermic reaction in which the transition state is very "product-like," namely, one in which a considerable amount of C−H bond formation has already taken place.

Several instances of *normal* isotope effects (including the one discussed above: (tmeda)Pt$(CH_2Ph)(H)Cl_2$ (**5**) in CD_2Cl_2, k_H/k_D = 3.1) for C−H reductive elimination have also been reported.[52,55,56,59] The data in Table 3 compare all the isotope effects that we have found for C−H reductive elimination; the table is arranged in the order of decreasing isotope effect. Not only do the values vary widely (some of this variation is of course due to differences in temperature), but they do not appear to correlate directly with the relative exothermicity of the reaction. The lack of correlation between these values suggests that reaction exothermicity alone cannot explain the discrepancy in isotope effects. Interestingly, for *all reported cases* of inverse isotope effects (entries 6−13), H/D exchange is observed between the alkyl (aryl) and hydride positions, constituting independent evidence for the presence of an intermediate preceding alkane loss. Thus, while H/D exchange does not *necessarily* lie on the reaction coordinate for reductive elimination, the data in Table 3 provide substantial support for such a link. It is still possible that σ-complexes mediate the reductive elimination of reactions which reveal normal isotope effects, but in these cases, the rate-determining step would involve formation of the σ-complex rather than dissociation of alkane from the metal center. That is, the transition state would lie much earlier along the reaction coordinate for C−H bond formation.

Table 3. Deuterium Kinetic Isotope Effects Measured for the Reductive Elimination of Alkanes from Various Alkylhydrido Transition Metal Complexes

entry	compd	temp (°C)	isotope effect	ref
	Normal Isotope Effects			
1	*cis*-$(PPh_3)_2$Pt(Me)(H)	−25	3.3	55
2	(tmeda)Pt$(CH_2Ph)(H)Cl_2$	−28	3.1	this work
3	*cis*-$(PPh_3)_2$Pt(CH_2CF_3)(H)	40	2.2	56
4	(P−P)Pt(CH_2CMe_3)(H)[a]	69	1.5	59
5	*mer*-$(PMe_3)_3$Rh(CH_2COCH_3)(H)Cl	31	1.3	52
	Inverse Isotope Effects			
6	$[Cp_2Re(CH_3)(H)]^+Cl^-$	9	0.8	67
7	(Cn)Rh$(PMe_3)(CH_3)$(H)	75	0.74	71
8	Cp*Ir(PMe_3)(Cy)(H)	130	0.7	64
9	$Cp_2W(CH_3)$(H)	73	0.7	68, 69
10	$Cp^*_2W(CH_3)$(H)	100	0.7	70
11	Cp*Rh(PMe_3)(3,5-$C_6H_3Me_2$)(H)	51	0.51	66
12	Cp*Rh(PMe_3)(Et)(H)	−30	0.5	65
13	(tmeda)Pt$(CH_3)_2$(H)Cl	−27	0.29	this work

[a] P−P = bis(dicyclohexylphosphino)ethane

We therefore believe that H/D exchange in (tmeda)Pt$(CH_3)_2$(H)Cl (**12**) supports the presence of a methane σ-complex that lies on the reaction coordinate for reductive elimination. Without an intermediate in this reaction, the inverse isotope effect would be very difficult to explain. The isotope effect for methane loss, then, is a composite value arising from an equilibrium isotope effect (reversible σ-complex formation) and a kinetic isotope effect (dissociation of alkane). Lack of direct observation of the σ-complex prevents us from deconvoluting this value.

Protonolysis of *trans*-$(PEt_3)_2$Pt(CH_3)Cl (15) in CD_3OD. We initially chose to evaluate the protonolysis of *trans*-$(PEt_3)_2$Pt(CH_3)Cl (**15**) because of the inverse isotope effect reported by Romeo *et al.*[99] Furthermore, **15** has been the subject of several protonolysis studies in the past,[27,28,99] and we wanted to compare its reactivity directly with our tmeda-ligated platinum complexes. Previous investigations utilized UV−visible spectroscopy to monitor the reaction, and clean isosbestic points suggested no intermediates were present in the reaction. However, upon investigating the protonolysis of **15** in CD_3OD by ^1H NMR, we observed deuterium incorporation into the methyl sites prior to methane loss (Scheme 4). Since there is no buildup of the intermediate responsible for this exchange, it would be invisible in the electronic spectrum. In contrast to

(93) Byers, P. K.; Canty, A. J.; Crespo, M.; Puddephatt, R. J.; Scott, J. D. *Organometallics* **1988**, *7*, 1363.
(94) Canty, A. J. *Acc. Chem. Res.* **1992**, *25*, 83.
(95) Goldberg, K. I.; Yan, J. Y.; Winter, E. L. *J. Am. Chem. Soc.* **1994**, *116*, 1573.
(96) Goldberg, K. I.; Yan, J. Y.; Breitung, E. M. *J. Am. Chem. Soc.* **1995**, *117*, 6889.
(97) Bigeleisen, J. *Pure Appl. Chem.* **1964**, *8*, 217.
(98) Melander, L. *Acta Chem. Scand.* **1971**, *25*, 3821.
(99) Romeo, R.; Minniti, D.; Lanza, S.; Uguagliati, P.; Belluco, U. *Inorg. Chem.* **1978**, *17*, 2813.

Scheme 10

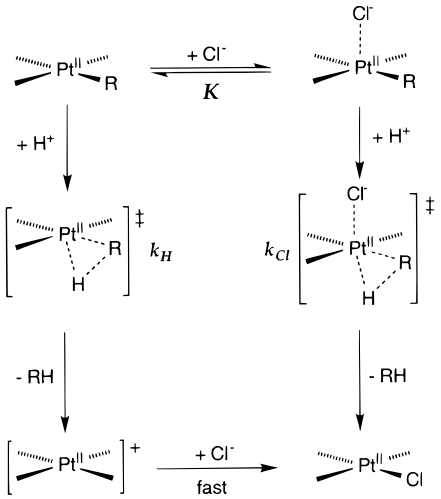

the protonolysis of (tmeda)Pt(CH_3)$_2$ (**11**), no platinum(IV) intermediate is observed; **15** and its isotopomers are the only species observed prior to elimination. We propose that deuterium incorporation results from the formation of an alkane σ-complex prior to methane dissociation.

Protonolysis of **15** might proceed via direct protonation at the platinum−carbon bond (see structures **B** and **C** above), or alternatively, it may proceed through a mechanism analogous to Scheme 8. In the latter case, the platinum(IV) intermediate would not be observed if it is less stable than the starting alkylplatinum(II) complex **15**. The former conclusion was favored by Alibrandi *et al.* in their extensive study of a series of alkylplatinum(II) species.[28] They propose a mechanism involving direct protonolysis of **15** through transition state **C** involving both chloride-dependent (k_{Cl}) and chloride-independent (k_H) pathways (Scheme 10). Nevertheless, we believe that a mechanism similar to Scheme 8, involving a phosphine-ligated alkylhydridoplatinum(IV) intermediate (**16**), is at least as consistent with the data, and also contributes to a more unified picture for the protonolysis of alkylplatinum(II) species (see below). Indeed, such a mechanism was proposed by Belluco and co-workers in their first study of the protonolysis of **15**.[27]

The proposed platinum(IV) intermediate, (PEt_3)$_2$Pt(CH_3)(H)Cl_2 (**16**), can in fact be observed in CD_2Cl_2. Although **16** appears to be less stable than (tmeda)Pt(CH_3)$_2$(H)Cl (**12**) (eliminating methane at −45 versus +10 °C, respectively, in CD_2Cl_2), its formation suggests that it might be an energetically viable (albeit unobserved) intermediate in methanol.

Unfortunately, the kinetic isotope effects are of little utility in identifying the correct mechanism. Because the reagents and the transition state leading to H/D exchange are virtually identical for the two mechanisms (reductive elimination forming a σ-complex versus direct electrophilic attack at the Pt−C bond), the isotope effect for H/D exchange ($k_H/k_D = 0.80$) is unable to distinguish between them. The isotope effect for methane loss is even more inverse ($k_H/k_D = 0.11$); this result merely suggests that formation of a strong C−H bond is nearly complete in this transition state.

Analysis: Common Mechanism? In this work we have evaluated the reactivity of four different systems: [1] (tmeda)Pt(CH_3)Cl (**2**) in methanol, [2] (tmeda)PtRCl (R = CH_3, CH_2Ph (**5**)) in dichloromethane, [3] (tmeda)Pt(CH_3)$_2$ (**11**) in methanol, and [4] *trans*-(PEt_3)$_2$Pt(CH_3)Cl (**15**) in methanol. Despite the significant differences among the systems, we believe all of the data support a common mechanism (Scheme 11): (1) chloride- or solvent-mediated protonation of Pt(II) (**V**)

Scheme 11

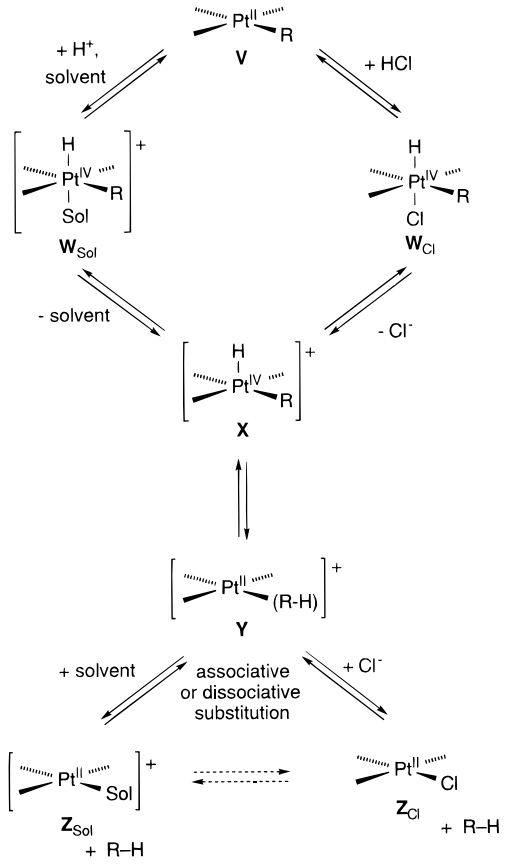

to generate an alkylhydridoplatinum(IV) intermediate (**W**), (2) dissociation of solvent or chloride to generate a cationic, five-coordinate platinum(IV) species (**X**), (3) reductive C−H bond formation producing an alkane σ-complex (**Y**), and (4) loss of alkane either through an associative or dissociative substitution pathway. Based on this proposal, the origin of the differences between the four systems lies in the fact that changing the solvent or the initial Pt(II) species alters the relative energy of the reagents, intermediates, and transition states, thereby changing the rate-determining step and/or dictating which intermediates may be observed.

This proposal also accounts for the differences in the chloride dependency of the reactions. Both the protonolysis of **2** in methanol and H/D exchange in **15** show positive dependence of the reaction rates on [Cl^-] (see Figures 2 and 11); however, the reactions still proceed with measurable rate in the absence of chloride. These results reflect the fact that formation of **W**, **X**, and **Y** may be mediated by either solvent or chloride, with chloride being a more effective mediator for these reactions than solvent.

On the other hand, *loss of methane* from intermediate **Y** in the protonolysis of **15** exhibits no measurable rate in the absence of chloride (Figure 11). This result suggests that alkane loss occurs via an *associative* chloride substitution pathway.

The reactions starting from an alkylhydridoplatinum(IV) intermediate (**6** in CD_2Cl_2 and **12** in methanol) exhibit an *inverse* dependence of the reaction rates on [Cl^-]. This result is most easily explained by pre-equilibrium chloride dissociation from $\mathbf{W_{Cl}}$ preceding the rate-determining step (see above). Because both H/D exchange and methane loss from **12** exhibit this inverse chloride dependence, we believe this reflects a *dissociative* substitution pathway, since an associative pathway, as observed for **15**, should cancel the chloride dependence.

Shown in Figures 14a−d are qualitative reaction coordinate

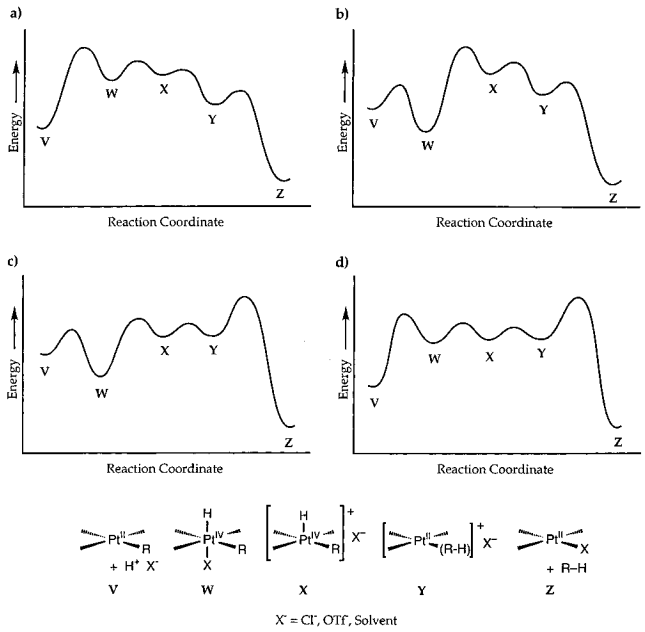

Figure 14. Qualitative reaction coordinate diagrams (based on Scheme 11) for the protonolysis reactions of (a**)** (tmeda)PtMeCl (**2**) in methanol, (b**)** (tmeda)PtMeCl (**2**) in dichloromethane, (c**)** (tmeda)$PtMe_2$ (**11**) in methanol, and (d**)** *trans*-$(PEt_3)_2$PtMeCl (**15**) in methanol. (See discussion in text.)

diagrams for each of the four systems analyzed. The diagrams, based on Scheme 11, account for the different observations made in each case. For the protonolysis of **2** in methanol, we obtain no direct evidence for intermediates in the reaction. Nevertheless, the data are still consistent with the mechanism proposed in Scheme 11 (Figure 14a). Although many specific features of the diagram remain speculative, the important details are the following: (1) the reagents are significantly more stable than any other species preceding the rate-determining step (i.e., only **2** is observed prior to product formation) and (2) the rate-determining step lies *before* dissociation of alkane from **Y**. Based on the [Cl^-] dependence of the reaction, we assign formation of **W** as the rate-determining step; such an energy profile reveals why no intermediates can be observed. It is also consistent with the observation that **14** is less susceptible to protonolysis than **2**, as generation of **W** from a cationic **V** should be more difficult.

Upon carrying out the same reaction in dichloromethane (rather than methanol), significant differences are observed. In this case alkylhydridoplatinum(IV) (**W**) is the most stable species under the reaction conditions. Although **W** is in rapid equilibrium with **V** prior to loss of alkane, it is the only species observed aside from the products (**Z**); Figure 14b reflects this change. The differences between Figures 14a and 14b can be accounted for by the change in solvent polarity, i.e., methanol is better able to stabilize the charged reagents and intermediates. Consequently, upon shifting to dichloromethane, the charged intermediate (**X**) and the preceding transition state become much less stable, thus making its formation the rate-determining step.

Protonolysis of (tmeda)$Pt(CH_3)_2$ (**11**) in methanol differs significantly from that of (tmeda)$Pt(CH_3)Cl$ (**2**). Although the only difference is replacement of chloride with a more electron-donating methyl group in the platinum coordination sphere, this change is apparently sufficient to stabilize Pt(IV) (**W**) relative to Pt(II) (**V**), because **W** becomes the species observed by ^1H NMR at low temperature. The other significant feature of this reaction is that alkane dissociation from the σ-complex (**Y**) is now the rate-determining step. Although **Y** is never seen directly, its existence is supported by deuterium incorporation into the methyl groups and the inverse isotope effect for methane loss (see above). These results are shown schematically in Figure 14c.

The protonolysis of $(PEt_3)_2Pt(CH_3)Cl$ (**15**) also exhibits some unique features. Again we believe the data are consistent with the mechanism proposed in Scheme 11 with the differences arising from the relative energy of the reagents, intermediates, and transition states (Figure 14d). As with the protonolysis of **11**, the rate-determining step is loss of alkane from the σ-complex (**Y**). In this case, however, no Pt(IV) intermediate (**W**) is observed; **15** is the species observed under the reaction conditions. This feature likely arises from the substitution of relatively "hard" amine donors (i.e., tmeda) with "soft" phosphine ligands. Soft ligands are commonly used to stabilize lower oxidation states. The relative energies of intermediates **W**, **X**, and **Y** remain unknown.

Despite the data that we have obtained for the four different systems, several detailed features of this mechanism remain uncertain. For example, although chloride loss precedes alkane reductive elimination, our kinetic data cannot distinguish between elimination from solvated six-coordinate and five-coordinate cationic intermediates. Furthermore, many aspects of the HCl oxidative addition mechanism remain unanswered. Although the reaction appears to proceed with *trans* stereochemistry (suggesting a heterolytic mechanism), it is not known whether the mechanism involves initial proton attack at Pt(II) followed by chloride association or the reverse order of addition. In the latter case, chloride or solvent are in fact necessary in order to generate the reactive five-coordinate intermediate (**X**). In the former case, however, **X** is rapidly trapped in a non-productive equilibrium by chloride or solvent. It must then be regenerated in a subsequent step prior to alkane elimination. Another area of uncertainty concerns the nature of the alkane σ-complex, because of our inability to observe this intermediate.

Conclusion: Implications for Alkane Activation by Pt(II)

We began this study hoping to gain insights into the mechanism of aqueous C−H activation by Pt(II), the microscopic reverse of the reactions discussed here. Based on our results, we believe we can now speculate further on some of the detailed aspects of this reaction. The mechanism for protonolysis of alkylplatinum(II) complexes involves a significant number of ligand association, dissociation, and substitution steps, and furthermore, the reaction proceeds through both ionic and neutral intermediates (Scheme 11). These features suggest an important role for the solvent (water) in Shilov's alkane oxidation system: it must be able to accommodate neutral and/or ionic intermediates in order to facilitate the various mechanistic steps. Significant stabilization *or* destabilization of any of the reaction intermediates relative to the others could dramatically decrease the rate of C−H activation. Interestingly, nearly all of the "electrophilic" alkane oxidation systems utilize highly polar solvents (H_2O, H_2SO_4, CF_3COOH).[4−7] This may be rationalized at least in part by comparing Figures 14a and 14b reading right-to-left—destabilization of ionic species in nonpolar solvent (Figure 14b) translates to a higher barrier for C−H activation.

The nature of the platinum ligands also appears crucial; they must be sufficiently labile to allow the various ligand exchange reactions to proceed at rapid rates. The initial interaction between the alkane and Pt(II) involves a ligand-substitution reaction (alkane for chloride or solvent). Although we cannot address whether the substitution takes place via an associative or dissociative mechanism, this step is likely the origin of chloride inhibition of alkane oxidation. In other words, chloride

competes favorably with alkane for a coordination site on Pt(II); that alkane can compete at all still seems quite remarkable. We cannot exclude the possibility that chloride plays a more intimate role in these processes as well, perhaps along the lines of structure **B** above as suggested by theoretical studies.[31]

Our results implicate the presence of *both* alkane σ-complexes and alkylhydridoplatinum(IV) as intermediates in the C−H activation reaction.[100] Contrary to our previous suggestion,[9] it appears that the alkylplatinum(II) species is generated by deprotonation of alkylhydridoplatinum(IV) (eq 1), *not* the σ-complex (eq 2). According to this proposal, the σ-adduct is an intermediate preceding the oxidative addition of the C−H bond. Such a mechanism is presumably facilitated by the accessibility of the Pt(IV) oxidation state. The other electrophilic alkane oxidation systems (such as those involving palladium or mercury) likely operate through a different pathway considering the significant instability of their M(IV) oxidation states.

Clearly these systems are highly complex, involving a number of intermediates. To date we have significant, but incomplete, understanding of how their relative stabilities and reactivities depend upon structure and reaction conditions. Studies continue toward our long-range goal: to exploit detailed understanding of the mechanism and energetics of electrophilic alkane oxidation for the rational design of improved catalysts.

Experimental Section

General Considerations. Protonolysis reactions involving **5** and **11** were carried out under an inert atmosphere using standard Schlenk techniques or in a glovebox, but for other reactions, this was unnecessary. ^{1}H and ^{2}H NMR spectra were obtained using General Electric QE300 and Bruker AM500 spectrometers. Low-temperature kinetics were obtained on the AM500 spectrometer using an automated sequence to record sequential spectra. NMR kinetics were all carried out in NMR tubes equipped with a screw cap and silicone/PTFE septum available from Wilmad Glass Co. Infrared spectra were recorded on a Perkin-Elmer 1600 series FTIR spectrometer. Solvents were dried prior to use: Et_2O-d_{10} over Na/benzophenone, CD_2Cl_2 over CaH_2 followed by 4 Å molecular sieves, and CD_3OD (and other isotopomers) over 4 Å molecular sieves. The following compounds were prepared according to literature procedures or analogous methods: (tmeda)$PtMe_2$ (**11**), (tmeda)PtMeCl (**2**), (tmeda)Pt(CH_2Ph)Cl (**5**), and *trans*-(PEt_3)$_2$Pt(CH_3)Cl (**15**), (4,4′-dimethyl-2,2′-bipyridyl)Pt(CH_3)$_2$ (**9**).[101,102]

^{1}H NMR Kinetics for the Protonolysis of (tmeda)PtMeCl (2) in CD_3OD. **2** (3 mg, 0.0083 mmol) and various amounts of LiCl and $LiClO_4$ were added to a series of NMR tubes according to the amounts determined for the particular experiment. For [Cl^-]-dependence experiments, the [LiCl] was varied between 0 and 0.66 M. For [H^+]-dependence experiments, [HOTf] was varied between 0 and 0.38 M. $LiClO_4$ was always added such that the ionic strength (μ = [HOTf] + [LiCl] + [$LiClO_4$]) equaled 1 M. This was followed by addition of the solvent (CD_3OD) containing a known amount of tBuOH as an integration standard. In order to monitor the kinetics at low temperature, the individual tubes were cooled to −78 °C prior to the addition of HOTf. After HOTf addition (total volume of reaction mixture = 700 μL.), the contents of the tube were mixed thoroughly (while keeping the tube as cold as possible), and the tube was then placed in the precooled NMR probe. After adjusting the necessary shims, a microprogram was initiated to automatically acquire spectra at regular time intervals. Spectra were then processed and integrated using WIN-NMR® software; the Pt−Me peak was integrated relative to the t*Bu*OH resonance. Data analysis was carried out using KaleidaGraph®.

Kinetic Isotope Effects for the Protonolysis of (tmeda)PtMeCl (2) in CD_3OD. See previous section for reaction details. The competitive isotope effect was measured by comparing the integration of CH_3D to CH_4 generated from the reaction carried out in a mixture of CD_3OD and CD_3OH. The non-competitive isotope effect was determined by comparing the rates of the reaction carried out in CD_3OH and CD_3OD.

Preparation of Alkylhydridoplatinum(IV) species (4, 6, 8, 10, 12, 16) in CD_2Cl_2. HCl(g) was dissolved in Et_2O-d_{10} (using a gas bulb containing a known amount of HCl) and the solution was then titrated to determine the HCl concentration. (An aliquot of the solution was added to a few milliliters of water containing phenolphthalein, and then titrated against a 0.100 N solution of NaOH.) Approximately 10 equiv of the HCl solution were added via syringe to a 5 mm NMR tube containing the appropriate alkylplatinum(II) reagent dissolved in CD_2Cl_2 at −78 °C. After mixing the contents while keeping the tube as cold as possible, the tube was placed in the precooled NMR probe. Relevant ^{1}H NMR data are recorded in Table 1.

^{1}H NMR Kinetics for the Reductive Elimination of Toluene from 6 in CD_2Cl_2. HCl/Et_2O-d_{10} (60 μL, 0.76 M) was added to a solution of **5** (4 mg, 0.0091 mmol) in CD_2Cl_2 at −78 °C. Pentachloroethane (4 μL) was also added as an integration standard. Sequential ^{1}H NMR spectra for the reductive elimination of toluene were obtained using the preprogrammed subroutine discussed above for the protonolysis of **2** in CD_3OD. The furthest downfield aromatic protons of **6** (δ 7.42 ppm , br s, 2 H) were integrated to obtain the kinetics data. A solution of HOTf was also prepared in Et_2O-d_{10} in order to monitor the [HOTf] dependence of the reaction; however, this solution had to be kept cold and used shortly after preparation to avoid its rapid decomposition at room temperature. A typical kinetics run involved adding HCl/Et_2O-d_{10} (25 μL, 1.88 M) to **5** (4 mg, 0.0091 mmol) dissolved in CD_2Cl_2 (0.5 mL) at −78 °C. After thoroughly mixing the solution at low temperature, HOTf/Et_2O-d_{10} (43 μL, 1.07 M) was added. The solution was again thoroughly mixed prior to placement in the precooled probe. To check the effect of a nonprotic Lewis acid, a solution of $SnCl_4$ in CD_2Cl_2 was prepared and was similarly added to a pre-formed solution of **6**.

Determination of Isotope Effects Involving 6 in CD_2Cl_2. Solutions containing DCl and mixed HCl/DCl solutions were prepared in a manner analogous to that described for HCl above. To obtain the equilibrium and overall kinetic isotope effects, the mixed HCl/DCl solution (130 μL, 2.09 M) was added to a solution of **5** (4 mg, 0.0091 mmol) in rigorously dried CD_2Cl_2 (0.5 mL), and the ratio of CH_4 and CH_3D was obtained by integrating the corresponding peaks in the resulting ^{1}H NMR spectrum. The syringe used to dispense the HCl/DCl solution was rinsed several times with approximately 100 μL of the solution to avoid complications arising from H/D exchange with the protic sites on the glass syringe. The ratio of HCl to DCl was calibrated by adding the solution (using the same pre-rinsed syringe) to an excess of CH_3Li·LiBr (relative to [H^+] + [D^+]) dissolved in THF-d_8. Integration of the CH_4 and CH_3D gave the HCl/DCl ratio, and this ratio was used to determine the equilibrium and kinetic isotope effects. Isotope effect and calibration experiments were typically done in triplicate.

^{1}H NMR Kinetics for H/D Exchange and Methane Elimination in 12 in CD_3OD. In an inert atmosphere glovebox, **11** (5 mg, 0.015 mmol) was loaded into a 5 mm NMR tube and then removed from the glovebox. CD_2Cl_2 (50 μL) was added to dissolve **11**, and the solution was then cooled to −78 °C. LiCl and $LiClO_4$ (of varying ratios depending on the experiment) were then dissolved in methanol (total solvent volume for reaction = 0.7 mL), and the solution was added to the cooled NMR tube. For [Cl^-]-dependence experiments, the [LiCl] was varied between 0.10 and 0.60 M for H/D exchange and between 0 and 0.80 for methane elimination. The ionic strength was held constant ([HOTf] + [LiCl] + [$LiClO_4$] = 1.21 M) for all the reactions. After thoroughly mixing the solution at low temperature, a triflic acid solution (in methanol) was added to the NMR tube. The solution was again mixed thoroughly before placing it in the precooled NMR probe to monitor the kinetics. The kinetics were monitored for both the H/D

(100) Independent work by Zamashchikov *et al.*[20] also supports the intermediacy of alkylhydridoplatinum(IV) in C−H activation; however, their argument is based on isotope effects and relies on the assumption that σ-complex formation would have no isotope effect. In light of strong evidence to the contrary (see refs 61−63), their conclusions appear open to question.

(101) Clark, H. C.; Manzer, L. E. *J. Organomet. Chem.* **1973**, *59*, 411.

(102) Appleton, T. G.; Hall, J. R.; Williams, M. A. *J. Organomet. Chem.* **1986**, *303*, 139.

exchange reaction and methane loss by integrating the Pt(IV)−Me resonance from **12** relative to an internal standard (pentachloroethane). The H/D exchange reactions were carried out in CD_3OD, while reactions involving methane loss were done in CD_3OH. Again preprogrammed subroutines were used to record the spectra; the program for monitoring methane loss included a solvent presaturation sequence to delete the −OH resonance.

^{1}H NMR Kinetics for H/D Exchange and Methane Loss from 15 in CD_3OD. In an NMR tube, **15** (5 mg, 0.010 mmol) was combined with the appropriate amount of LiCl and $LiClO_4$ (ratio varied depending on the experiment). The ionic strength was held constant ([HOTf] + [LiCl] + [$LiClO_4$] = 1.15 M) for all experiments. In order to determine the [Cl^-] dependence of the reactions, [LiCl] was varied between 0.10 and 0.50 M for H/D exchange and between 0.067 and 0.78 M for methane elimination. The reagents were dissolved in methanol (CD_3OD for monitoring H/D exchange and CD_3OH for methane loss) and then cooled to −78 °C. After addition of a methanol solution of triflic acid (DOTf/CD_3OD for H/D exchange and HOTf/CD_3OH for methane loss), the reaction was mixed thoroughly and then placed in the NMR probe. Kinetics data were obtained by monitoring the loss in the integration intensity of the Pt−Me resonance relative to an internal standard (pentachloroethane). Again preprogrammed subroutines were used to record the spectra; the program for monitoring methane loss included a solvent presaturation sequence to delete the −OH resonance.

Kinetic Isotope Effects for H/D Exchange and Methane Elimination from 12 and 15 in Methanol. Kinetic isotope effects for H/D exchange and methane elimination from **12** in CD_3OD were obtained by comparing these rates with those of analogous reactions of **12-d_6** in CH_3OH and CH_3OD, respectively. Standardized solutions of HOTf in CH_3OH and DOTf in CH_3OD were prepared for these reactions. Reaction conditions were identical to the reactions carried out in CD_3OD. Reactions involving **12-d_6** were monitored by ^{2}D NMR, and again spectra were accumulated automatically. Kinetic data were obtained by monitoring the loss in the integration intensity of the Pt−CD_3 resonance relative to an internal standard (toluene-d_8). When monitoring elimination of CD_4 in CH_3OD, the solvent resonance was suppressed using the "1−3−3−1" pulse sequence developed by Hore.[103,104]

Isotope Effect for Protonolysis of "[$PtMeCl_3$]$^{2-}$" in Water and Methanol. The dry reagents [NMe_4]$_2$[$PtMeCl_5$] (100 mg, 0.19 mmol) and $CrCl_2$ (46 mg, 0.37 mmol) were combined and thoroughly mixed in a small flask equipped with a stirbar. The flask was placed on the high-vacuum line, evacuated, and cooled to liquid N_2 temperature. A 10:1 mixture of degassed D_2O:H_2O was then condensed into the flask and allowed to warm. Upon thawing, the solution turned dark green (reaction with Cr(II)) and gas evolution was immediately apparent along with formation of a black precipitate. The gas was collected and quantified using a Toepler pump, and the CH_4/CH_3D mixture was characterized and their ratio determined using ^{1}H NMR spectroscopy. Alternatively, the dry reagents were loaded into an NMR tube equipped with a J. Young valve (Wilmad Glass Co.) under inert atmosphere. Methanol was then vacuum transferred into an NMR tube at −78 °C. The heterogeneous mixture was mixed while warming to 0 °C. Methane evolution was again immediately apparent along with formation of black precipitate. The methane generated was analyzed by vacuum tranfer of all volatiles into a separate NMR tube.

Acknowledgment. This work was supported by the Office of Naval Research and the Army Research Office. S.S.S. thanks the National Science Foundation for a predoctoral fellowship.

JA960110Z

(103) Hore, P. J. *J. Magn. Reson.* **1983**, *54*, 539.
(104) Hore, P. J. *J. Magn. Reson.* **1983**, *55*, 283.